Midterm Tower Design Project

Andrew Lunyk, Spencer Kirsch, Myisha Hassan, Joseph Sutton

The Cooper Union for the Advancement of Science and Art

ME 408: Introduction to Computer Aided Engineering

Professor Scott Bondi

November 11, 2024

Table of Contents

INTRODUCTION

The goal of this project was to design a 525-foot wind turbine tower for Enercon's 9.25 MW model, optimized for minimum cross-sectional area and mass while meeting specific performance and safety requirements.

The design analysis was conducted with assumptions of constant air density, consistent wind load, and 316 Stainless Steel as the construction material, assumed to be linear, elastic, isotropic, and homogeneous. Also, the ground was considered rigid, and the tower's baseplate was modeled as fully fixed and bolted to the foundation. For the analysis, the tower was modeled as a cantilever beam with the base fully fixed to a stationary concrete foundation, reflecting real-world constraints. Additional engineering assumptions include ignoring the load from power generation, as it is negligible compared to the other loads under consideration.

The design accounts for environmental conditions at the installation site, including normal operating wind speeds of 70 mph, extreme gusts up to 135 mph, and temperatures ranging from -10°F to 135°F, with turbine operation at 6 to 12 rpm. For safe operation, the tower was designed to avoid natural frequency ranges that could lead to resonance if a blade detaches.

Using ANSYS Workbench, simulations and calculations for deflection, stress distribution, factor of safety, natural frequency modes, and buckling were conducted. The results confirmed that the optimized tower structure meets all structural and thermal constraints with minimized material usage.

GEOMETRY

For hand calculations and verification of simulations, the tower is approximated as a hollow beam with a constant circular cross-section, fixed to the ground. This circular beam has an outer radius of 36 ft and an inner radius of 35 ft. The blades are modeled as rectangular surfaces, each 217 ft in length with an average width equal to 1/12 of the length, subjected to wind pressure.

The simulation geometry models the final tower design as a straight cylindrical base up quarter of the height and then a tapered cylindrical structure, with the cross-section decreasing with height to the top. A simplification was made—wind turbine towers consist of multiple steel sections bolted together to form a conical shape, but for this model, the tower is represented as a single, continuous piece of extruded steel, reducing model complexity.

Three tower designs were developed, each serving a different purpose in the analysis and optimization process. The first design, a straight hollow cylinder, is a simple cylindrical tower with a uniform cross-section, created specifically for initial hand calculations. The second design, fully tapered, is a tower with a tapered cylinder decreasing in radius upwards and structural analyses were performed using Python-based code. Lastly, the Hybrid Cylinder-Tapered design served as the optimized tower model, with a straight cylindrical base for the first quarter of the height, followed by a tapered section toward the top. This final design was refined to achieve reduced volume and mass.

The initial hollow cylinder model served as a reference in developing the final geometry of the tower. Based on moment of inertia calculations related to deflection, the minimum required moment of inertia was found to be 7103 ft^4. Using Desmos for optimization (see Appendix I), a feasible cross-section for the hollow cylinder was identified. This cross-section, with an outer diameter of 36 ft and an inner diameter of 35 ft, resulted in a moment of inertia of 8786 ft^4. To simplify manufacturing, only whole-number dimensions were chosen, which led to a slight deviation from the calculated minimum, as achieving a moment of inertia close to 7103 ft^4 would have required non-rounded values. A preliminary simulation with this cross-section was conducted to evaluate deflection and stresses under both extreme and typical wind conditions at ambient temperature. The results aligned with the theoretical deflection calculation for the cylinder (1.42 ft). However, during review, it was noted that some boundary conditions were missing - standard gravity was not applied, the nacelle's weight on the tower was omitted, and the wind pressure on the tower surface was modeled as a remote force instead of a horizontal pressure component.

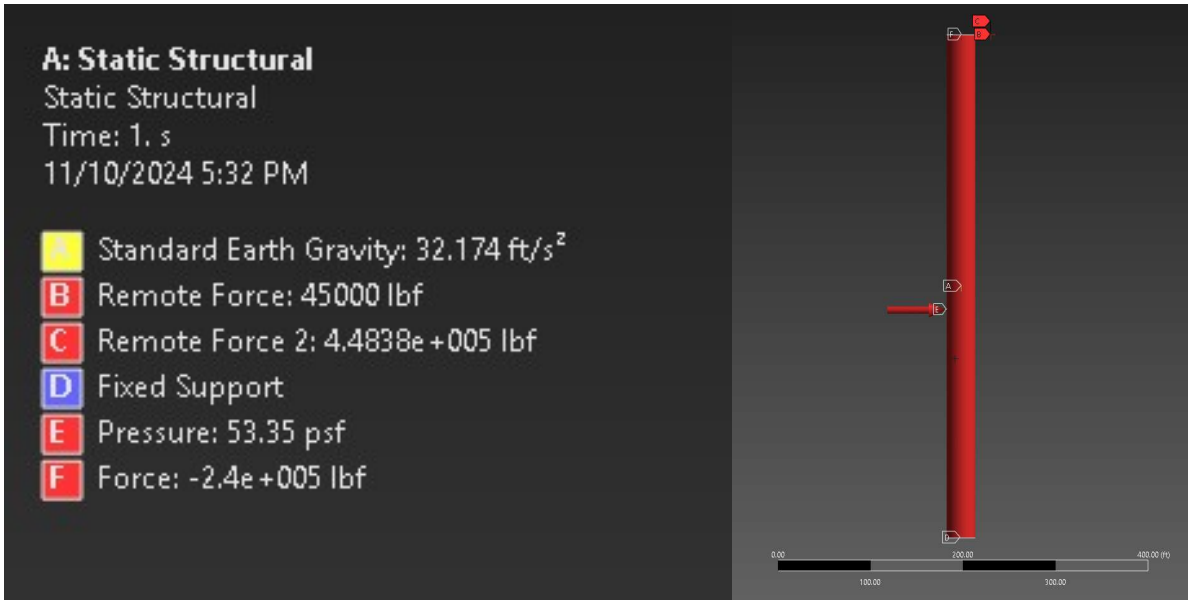

Figure 1: Corrected Boundary Conditions for Hollow Cylinder Simulation

With the updated conditions applied in the simulation in Figure 1, the von Mises stress criterion was surprisingly met, even accounting for fatigue; however, the deflection did not meet the requirements. The maximum allowable stress should be 23,733 psi with a maximum deflection of 1.42 ft. For this initial simulation, the results indicated a maximum stress of 21,440 psi but a deflection of 3.19 ft shown in Figure 2 and 3.

Figure 2: Von Mises Stresses Under Extreme Wind Conditions and Ambient Temperature of Hollow Cylinder

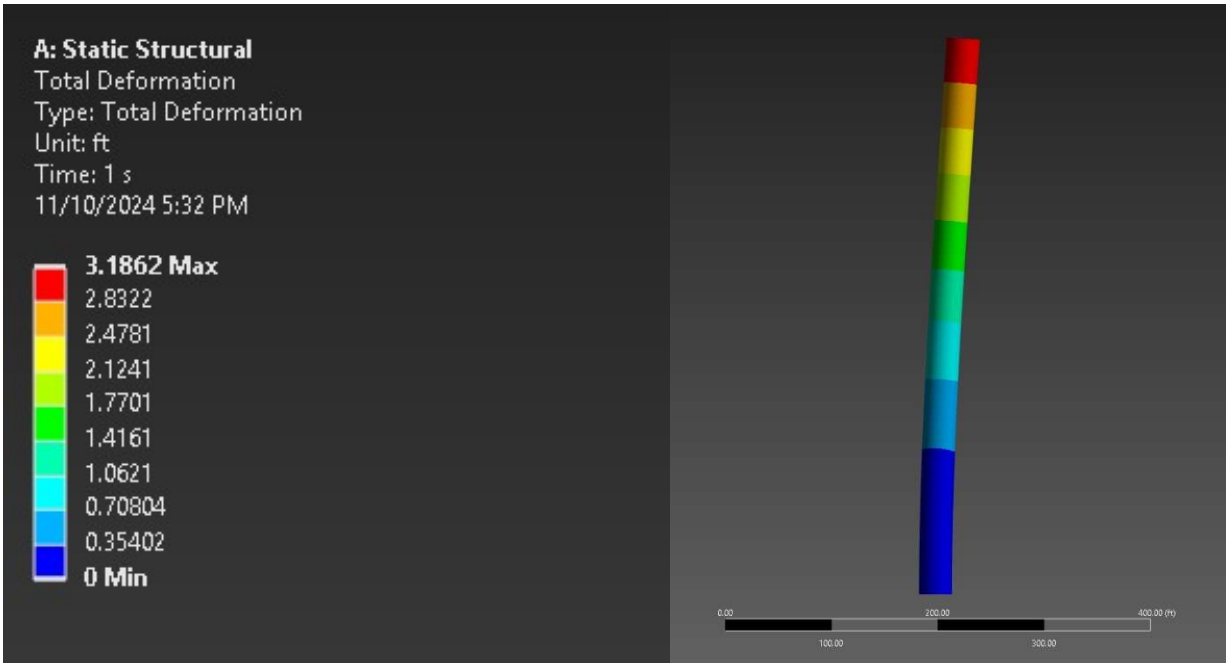

Figure 3: Deflections Under Extreme Wind Conditions and Ambient Temperature of Hollow Cylinder

This error was identified relatively late in the design process, so the original simulation was used as a reference for selecting the geometry. Variations in outer and inner diameters within the 30-40 ft range were explored, and simulations with a tapered section were conducted. While the tapered sections showed efficiency, they did not result in substantial volume or mass savings. This led to consideration of a hybrid design—using a hollow cylinder for the first quarter of the tower's height, with a slimmer tapered section for the remaining three-quarters. This design choice allowed for greater volume savings by ensuring the lower portion of the tower was strong enough to withstand the moments generated by the offset blades and wind. By using a hollow cylinder near the base, the design could better support these forces. The remaining height featured a linear taper that could be slimmer since it was less impacted by the moment. This approach was more effective than a fully tapered section from the base, as the taper rate would have to be slower to cover the entire height, resulting in more volume. Despite referencing dimensions from an incorrect simulation, a viable section option was identified. Detailed CAD drawing of final tower design is shown in Figure 4 and tower dimension overview tabulated in Table 1.

Table 1: Dimensions of Final Tower Design

	Hybrid Cylinder-Tapered Tower
Top Outer Diameter [ft]	9.66
Base Outer Diameter [ft]	33
Tower Wall Thickness [ft]	2
Baseplate Outer Diameter [ft]	37
Baseplate Thickness [ft]	3
Footprint [ft^2]	4300
Cross-Sectional Area [ft^2]	12731

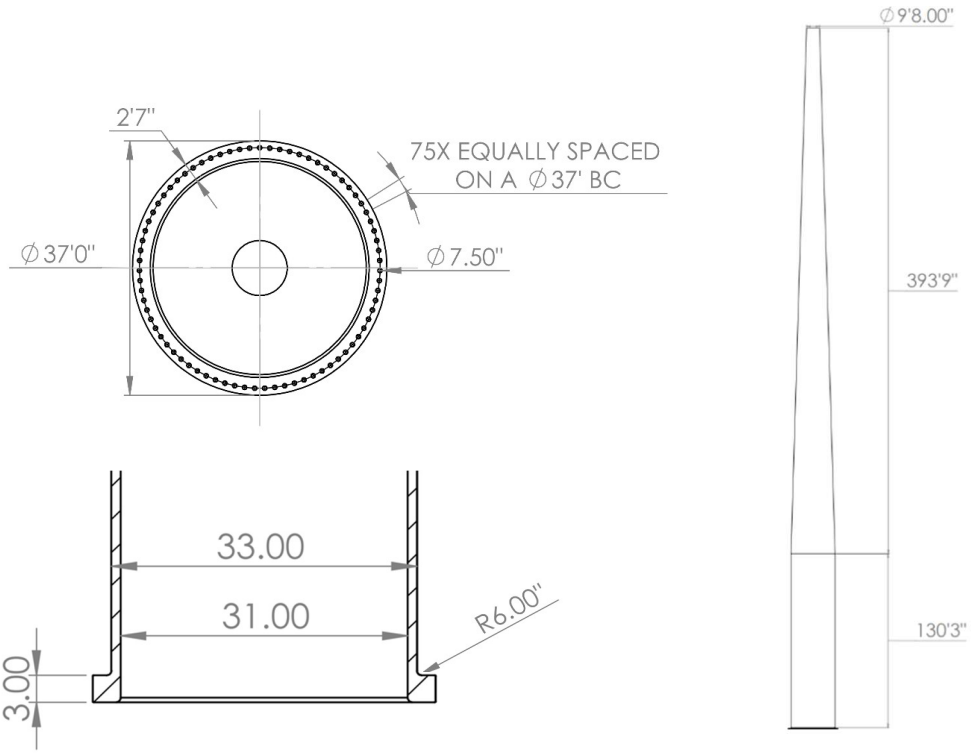

Figure 4: Dimensioned Drawing of Hybrid Cylinder-Taper Tower

Table 2: Properties of Tower Designs

	Straight Hollow Cylinder Tower	Hybrid Cylinder-Tapered Tower
Mass [lbm]	12,324,664	14,898,269
Volume [ft^4]	29,275	30,793
Moment of Inertia [ft^4]	8786	16081

When comparing the hybrid design to the hollow cylinder in Table 2, it may initially appear that the selected design was not fully optimized, as it resulted in increased volume and mass. However, it is important to consider that while the hollow cylinder minimized volume and mass as much as possible, it did not meet the deflection criteria. In contrast, the hybrid design only differed by around 1,500 cubic feet in volume and approximately 2 million pounds in mass from the hollow cylinder, while meeting both deflection and stress requirements. Additionally, it's worth noting that the moment of inertia of the hybrid cylinder is almost twice as large than the theoretically calculated minimum value needed to meet the deflection criteria, suggesting a potential error in the initial calculation. Despite referencing incorrect values, the design choices based on these initial calculations effectively mitigated stress and deflection issues. Further discussion of this will be provided in the results section.

MODELING

Table 3 outlines the weather conditions used for the simulation scenarios, covering both typical and extreme environmental conditions that the wind turbine may encounter. The 'Normal Condition' represents standard operating parameters, including typical wind speed and a midpoint (ambient) operating temperature within the expected range. The 'Extreme Condition' tests the tower under the peak wind speeds combined with a midpoint temperature.

Table 3: Weather Conditions for Simulations

	Wind Speed [ft/s]	Temperature [°F]
Normal Condition	102.7	62.5
Extreme Condition	198.0	62.5

The structural analysis of the wind turbine tower was conducted in Ansys Workbench, with material properties for 316 Stainless Steel provided as an input geometry parameter (material properties shown in Table 4. For deflection, maximum stress, and buckling failure analyses, only the 'Normal Condition' and 'Extreme Condition' were used, reflecting the typical and peak wind speeds the tower may experience. The loads and boundary conditions applied to the tower model under these conditions are shown in Table 5, Figure 5, and Figure 6.

The extreme temperature conditions (-10°F and 135°F) are analyzed separately, without any applied loads, to assess the thermal effects on the tower's vertical deformation due to temperature changes. These temperature extremes do not influence the magnitude of wind or weight-based loads, as temperature variations primarily cause material expansion and contraction rather than modifying these forces.

Table 4: Material Properties of 316 Stainless Steel

Material Property	Value
Modulus of Elasticity E	$29 * 10^3$ ksi
Poisson's ratio v	0.3
Coefficient of Thermal Expansion α	$9.6 * 10^{-6}$ in/in°F
Density ρ	490 lbm/ft^3

Table 5: Magnitudes of Applied Loads on Tower

	Normal Condition	Extreme Condition
Wind Pressure Distributed Load on Tower [lbf/ft^2]	14.3	53.4
Point Force due to Wind on Blades [lbf]	120,560	448,380
Moment caused by Weight of Blades [lbf·ft]	1,440,000	
Weight of Nacelle [lbf]	240,000	
Weight of 3 Blades [lbf]	45,000	

For both normal and extreme operating conditions, the applied loads and boundary conditions included the weight of the nacelle, an offset moment from the blades' weight, distributed wind pressure along the tower, a point load from wind acting on the blades, downward gravity (32.2 ft/s^2) to account for the tower's weight, and a fixed support at the tower's base.

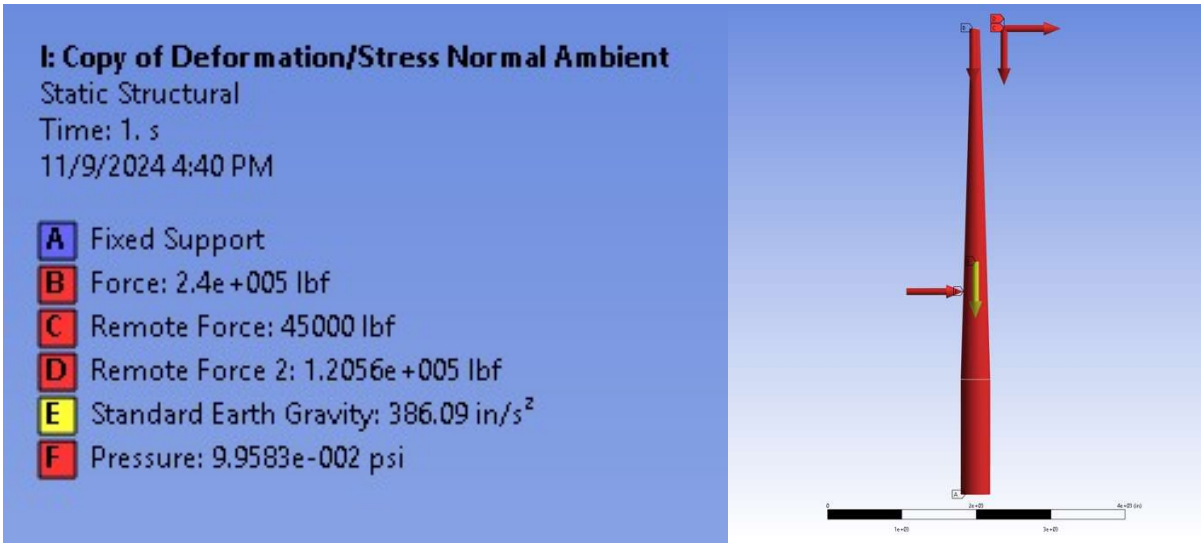

Figure 5: Boundary Conditions and Constraints for Normal Conditions

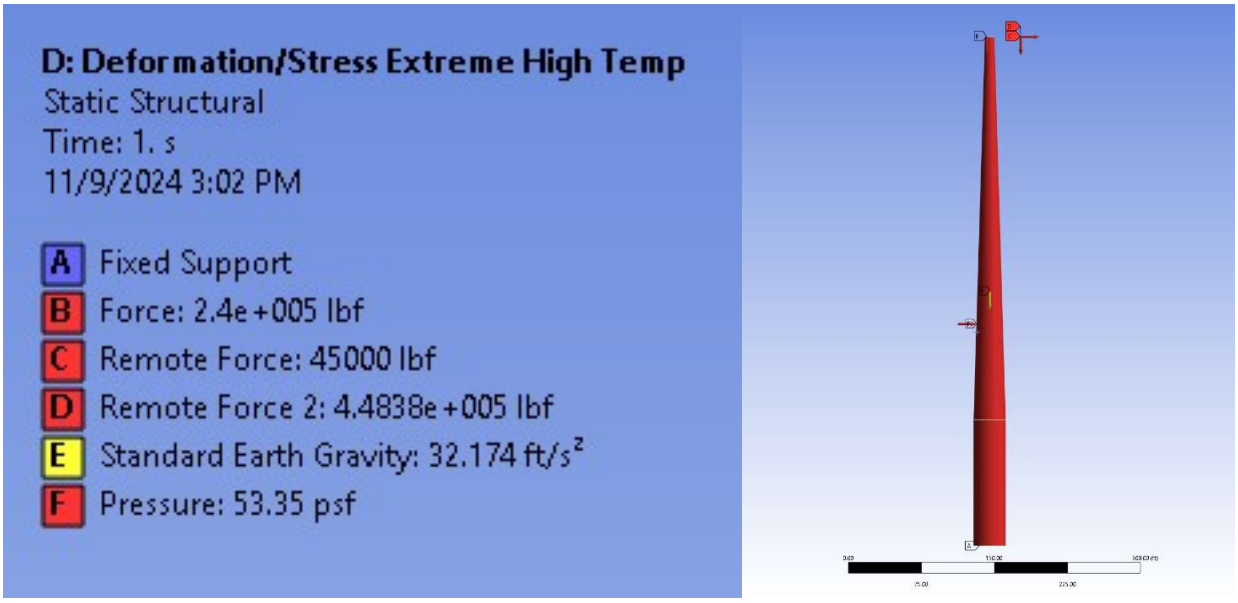

Figure 6: Boundary Conditions and Constraints for Extreme Conditions

MESHING

To achieve a fine mesh, the tower and flange were modeled separately. When meshing them as a single body using the multizone hexa/prism method with a relatively small element size, the mesh would consistently fail around the filleted area of the flange. This outcome is expected, as tetrahedral elements are generally better suited for curved surfaces. However, applying a tetrahedral mesh to the entire tower would significantly increase analysis time, as a much higher element count is required to maintain fine mesh quality compared to the multizone hexa/prism method. A hexa/prism multizone mesh with a 1-foot element size was selected for the tower, as it allows for a high-quality mesh with fewer elements, ultimately reducing analysis time and improving the accuracy of stress results. The final mesh used is shown in Figure 7 and 8.

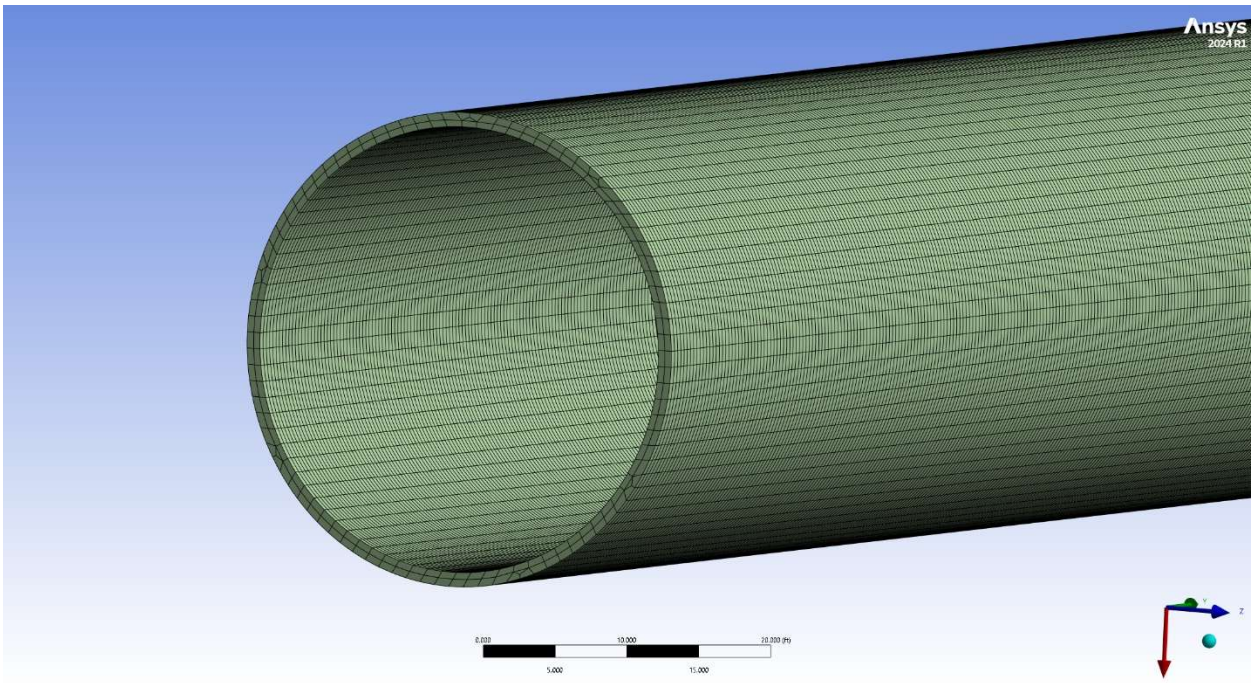

Figure 7: Multizone Hexa/Prism Mesh (Base of the Tower)

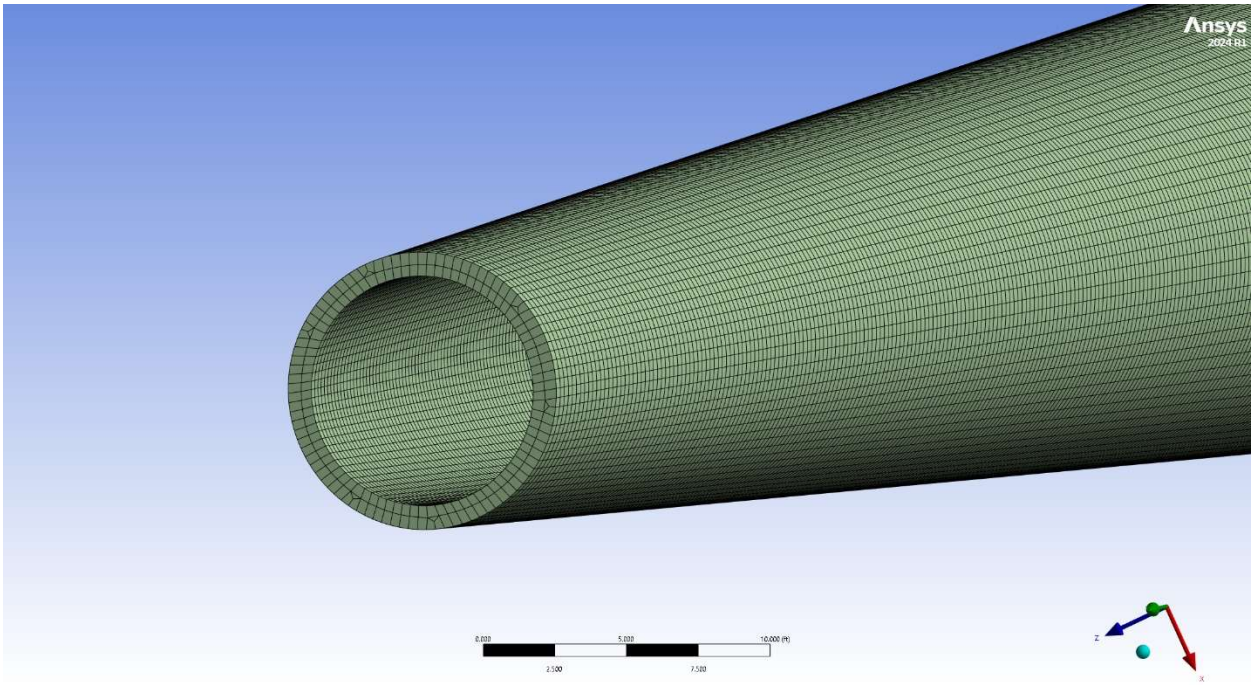

Figure 8: Multizone Hexa/Prism Mesh (Top of the Tower)

RESULTS

Table 6: Tower Design Results Comparison

	Hand Calculation		FEA Simulation	
	Straight Cylinder		Hybrid Cylinder-Tapered	
Weather Condition	Normal	Extreme	Normal	Extreme
Max Deflection [in]	**3.7**	**13.6**	**4.5**	**16.5**
Max Tower Stress [ksi]	**2.0**	**7.2**	**6.4**	**12.0**
Buckling Load Failure Multiplier	**31**		**95**	
Natural Frequency: 2 blades [rpm]	**21**		**32**	
Thermal Effects: Tower Height Change for -10°F [in]	**-4.4**		**-5.0**	
Thermal Effects: Tower Height Change for 135°F [in]	**4.4**		**3.6**	

The results from the simulation of the hybrid cylinder-tapered design and the hand calculations for both the straight cylinder and fully tapered designs closely match, remaining

within the similar order of magnitude as shown in Table 6. This alignment validates the hand calculations as a reliable verification of the FEA simulations.

Additionally, all results meet the specified structural and frequency constraints. Under normal operating conditions, the maximum deflection does not exceed 1.05 ft or 12.6 in (L/500), and under worst-case conditions, it remains below 1.42 ft or 17 in (L/370). The factors of safety for maximum stress exceed 1.65, meeting the required threshold for material failure, and the factors of safety for buckling exceed 8, fulfilling the constraint for buckling resistance. Furthermore, the natural frequencies of the tower, even in the event of a blade detachment, lie outside the operating frequency range of the rotating turbine blades (6 to 12 rpm), allowing for safe shutdown.

Maximum Stress

The yield stress of 316 Stainless Steel is 42 ksi; however, with fatigue considerations, the effective yield stress of the construction material is reduced to 39 ksi. A minimum factor of safety of 1.65 was applied to this value, establishing the maximum allowable stress for the tower structure at 23.7 ksi. For the connection hardware, a stricter factor of safety of 6 was required, limiting the maximum allowable stress on these components to 6.5 ksi.

The maximum stress on the tower is expected to be at the base due to the combined effects of axial loads and bending moments. By superimposing the uniform stress distribution from centric loads with the linear distribution from bending, the maximum stress distribution was determined for eccentric loading conditions.

The maximum normal stress on the tower includes both bending and axial stress components. Bending stress arises from the bending moment at the base, which is generated by the combined effects of the offset weight of the blades, wind pressure acting on the tower surface, and wind force on the blades. Axial stress is due to the total deadweight acting on the tower, comprising the weight of the nacelle and blades, applied as a point load at the tower's top.

$$\sigma_{max} = \sigma_{bending} + \sigma_{axial} = \frac{My}{I} + \frac{P}{A}$$

The calculated maximum stress was 2.0 ksi and 7.2 ksi for normal and extreme weather conditions, respectively (calculations shown in Appendix I). Table 7 tabulates the simulation results for maximum stress, which is shown to be below the maximum allowable stress for tower structure material (23.7 ksi). Figure 9 and Figure 10 provide general images of the tower's von Mises stress distribution. Close-up views highlighting the compressive and tensile sides of the tower's von Mises stress are available in Appendix III.

Table 7: Maximum Stress of Tower Under Different Conditions

	Normal Conditions [ksi]	Extreme Conditions [ksi]
Hybrid Cylinder-Tapered	6.4	12

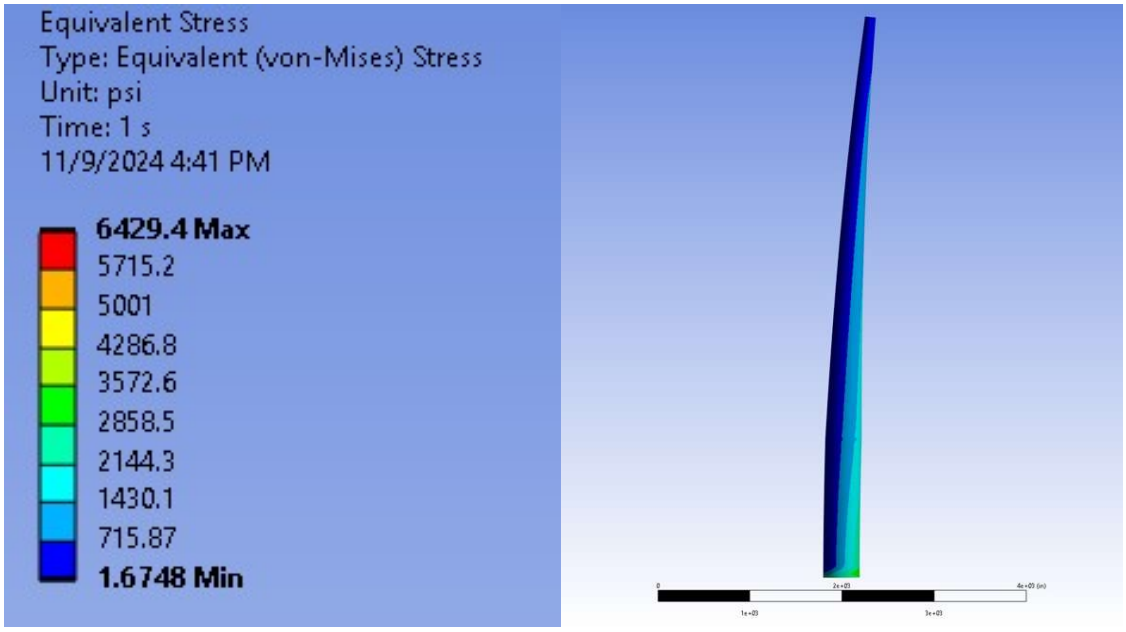

Figure 9: Von Mises Stress under Normal Conditions

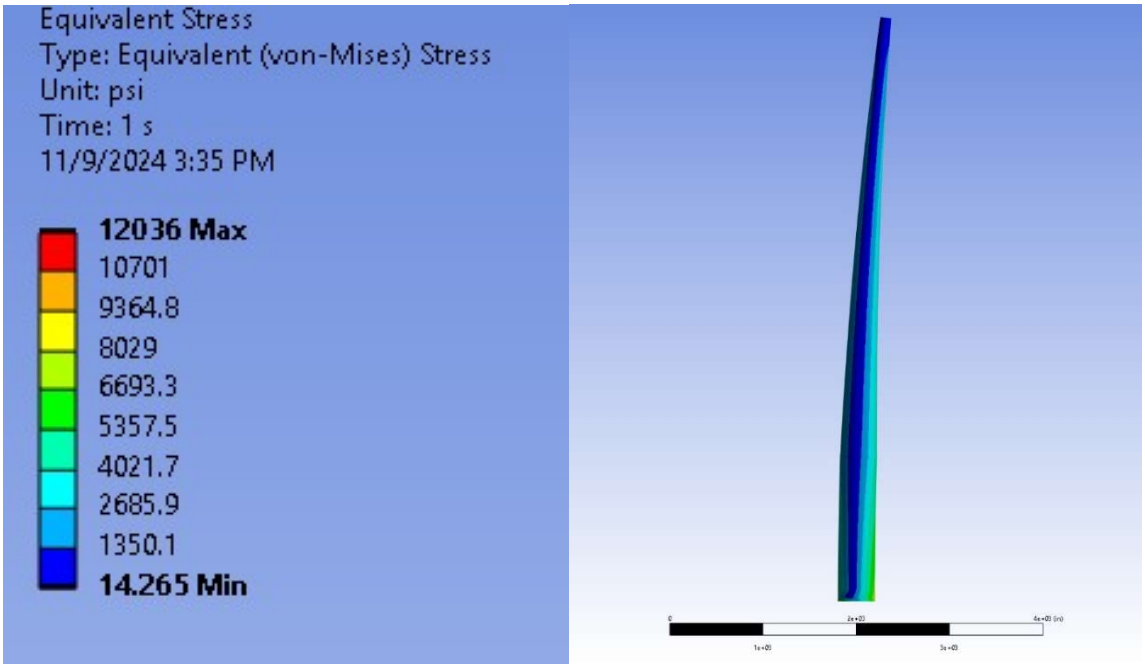

Figure 10: Von Mises Stress under Extreme Conditions

Maximum Deflection

The maximum deflection was caused by the force from the wind pressure acting along the tower (w_x), the force from the wind on the blades (P_x), and the moment caused by the weight of the blades (M_y). These combined forces contribute to a deflection calculated using the equation:

$$\delta_{max} = \frac{8P_xL^3 + 3w_xL^4 + 12M_yL^2}{24EI}$$

The design criteria specify that maximum allowable deflection should not exceed 1.05 ft (12.6 in) under normal operating conditions and 1.42 ft (17 in) under extreme weather conditions. Hand calculations for a straight hollow cylinder design yielded deflections of 0.31 ft (3.2 in) and 1.13 ft (13.6 in) under normal and extreme conditions, respectively. These values are well within the allowable limits, indicating that the straight cylinder design would likely meet the deflection requirements.

Running, FEA simulations shown in Figure 11 and 12, the deflection results for the hybrid cylinder-tapered design under normal conditions showed a slightly higher value of 4.5 in, still within the acceptable range but indicating an increase compared to the straight cylinder. Under extreme conditions, the hybrid design exhibited a deflection of 16.5 in, approaching the upper allowable limit but still compliant with design constraints.

Table 8: Tower Deformation Under Different Conditions

	Normal Conditions [in]	Extreme Conditions [in]
Hybrid Cylinder-Tapered	4.5	16.5

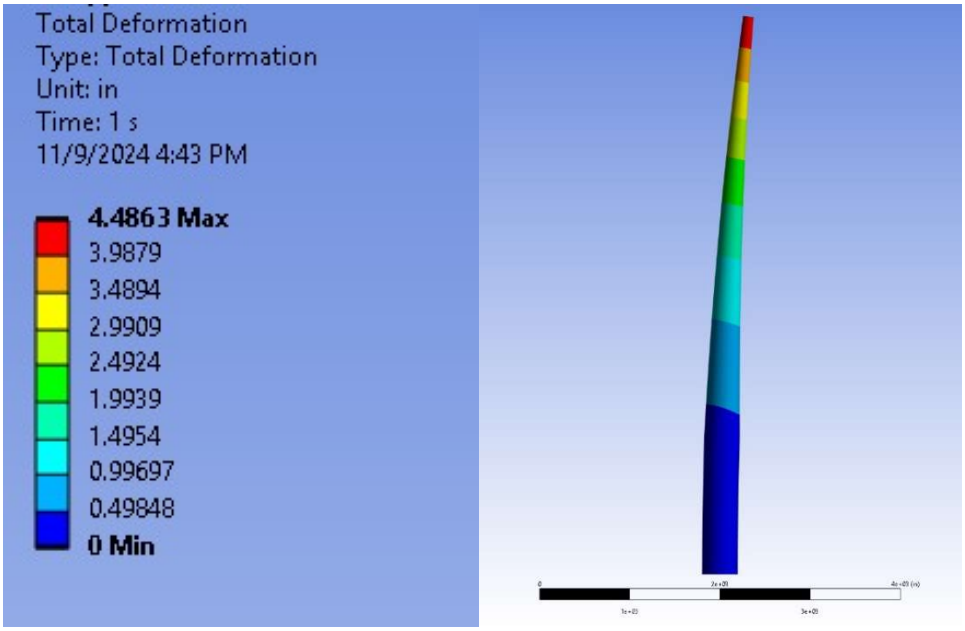

Figure 11: Total Deformation under Normal Conditions

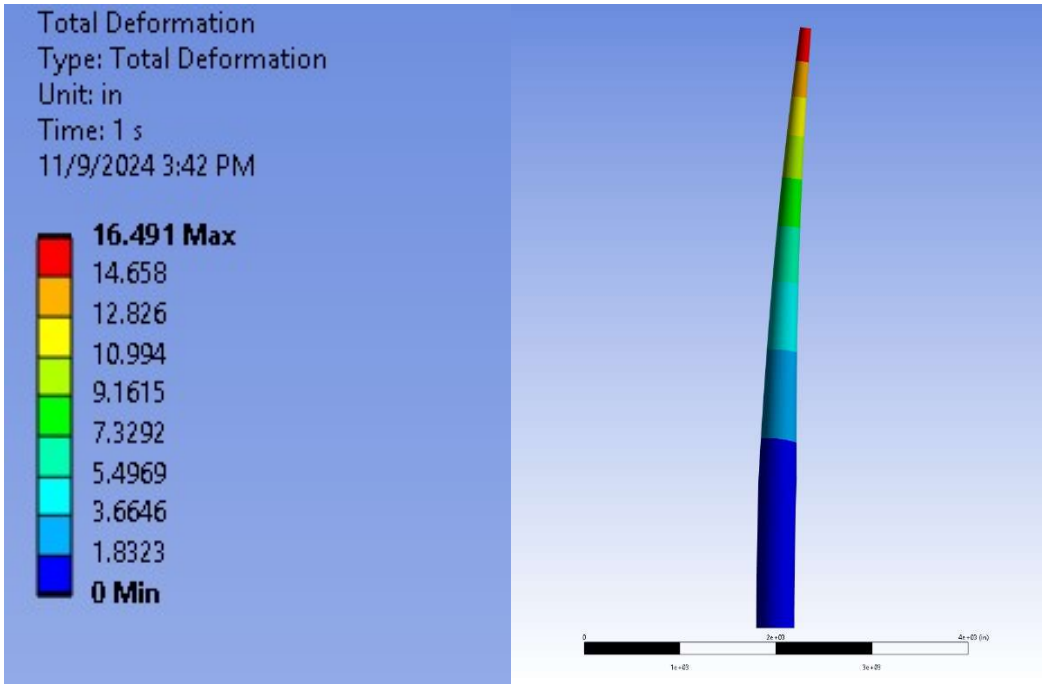

Figure 12: Total Deformation under Extreme Conditions

Thermal Effects: Tower Height

The site's temperature range, varying from -10°F to 135°F, causes the wind turbine tower to expand or contract due to thermal effects. Assuming thermal deflection of the tower due to thermal effects behaves as a linear expansion of a solid body, the vertical expansion or contraction can be calculated. Using the thermal expansion formula,

$$\Delta L = \alpha L(\Delta T)$$

where α is the coefficient of thermal expansion for 316 Stainless Steel (9.61×10^{6} in/in°F), ΔT is temperature difference the tower will experience in stages: from 135°F to ambient (62.5°F), and then from ambient to -10°F, and L is the initial height of the tower, the maximum expected vertical change in height over the full temperature range can be determined. The hand calculation results based on the temperature fluctuations are shown in Appendix I. Table 9 shows the FEA simulation results for the tower design deformation due to thermal effects.

Table 9: Maximum Thermal Expansion and Contraction of Tower Design

	Height Change at -10°F [in]	Height Change at 135°F [in]
Hybrid Cylinder-Tapered	-5.0	3.6

The changes in tower height due to thermal effects are minimal, with hand-calculated thermal deformation results (magnitude of 4.4 inches) closely aligning with simulation values for the final design. This consistency further validates the robustness of the design approach.

In the FEA simulation, the tower was analyzed for directional deformation along the y-axis using only the thermal conditions and gravitational load. The thermal effects analysis excludes external loads from wind or operational forces (the extreme and normal weather conditions) to isolate the impact of temperature-induced material expansion or contraction, to clearly see the tower height change due to the extreme temperature changes (-10°F and 135°F) alone.

The results show that while the straight cylinder design offers lower deflection values, the hybrid cylinder-tapered design optimizes material usage with slightly higher, but acceptable, deflection under both normal and extreme conditions. The close alignment of hand calculations and simulation results also validate the accuracy of the applied equation and assumptions in finding the deflection under combined loading conditions.

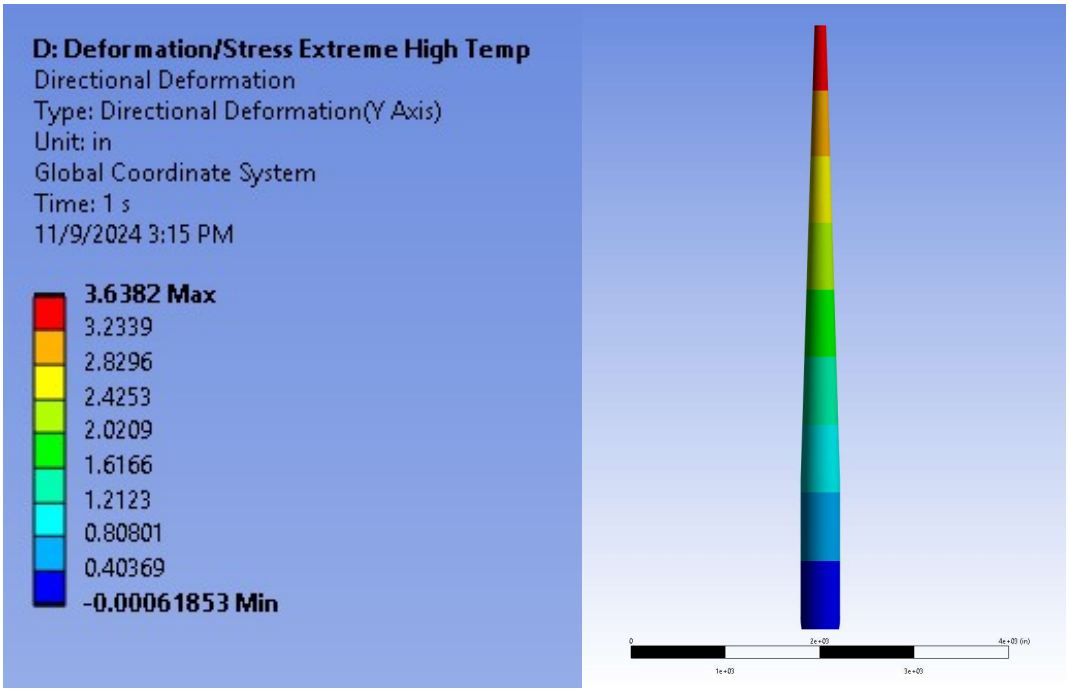

Figure 13: Expected Tower Height Change due to Temperature of 135°F

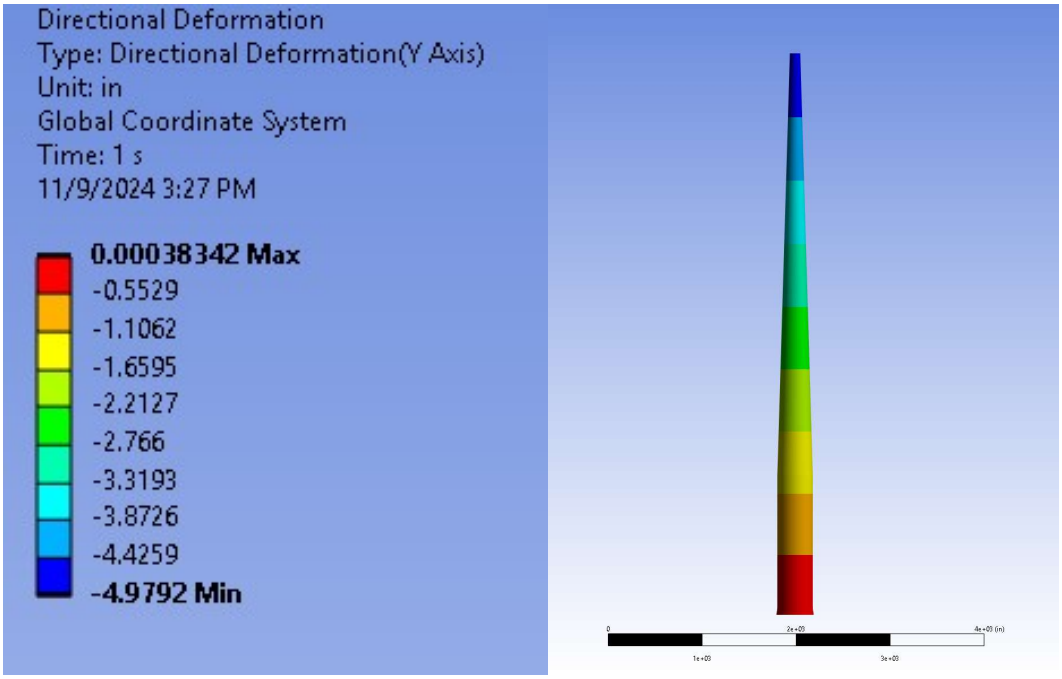

Figure 14: Expected Tower Height Change due to Temperature of -10°F

Natural Frequency:

The tower's natural frequency must be kept outside the turbine's operating frequency range of 6 to 12 rpm to prevent resonance-induced structural damage over time. In the event of a blade detachment, the remaining two blades exert an uneven, cyclic force that may potentially excite the tower's natural frequency, so it is essential to ensure that the frequency of this force does not align with the tower's natural frequency.

Having only two blades can create uneven loading, which might lead to periodic forces that could excite the tower's natural frequency. However, this isn't due to a significant change in the natural frequency itself but rather due to the asymmetrical loading pattern that can amplify oscillations if the natural frequency were within the operating range. Ensuring the natural frequency of the tower remains well outside the operating range provides a safety margin against oscillatory amplification due to these potential cyclic forces.

The natural frequency of the tower-nacelle system was calculated by treating the tower as a cantilever beam with a concentrated mass at its free end, representing the nacelle. To account for the distributed mass of the tower, an effective mass approximation was used, where 23% of the tower's mass was added to the nacelle mass; this allowed the tower's distributed mass to be represented as if a portion were concentrated at the top. The mass of the blades was excluded from the calculation, as their effect on the natural frequency is minimal due to their relatively low mass compared to the tower and nacelle and their rotating motion, which does not directly contribute to the tower's vertical vibration modes.

The resulting effective mass, $m_{Total} \cong m_{nacelle} + 0.23m_{tower}$, was used to estimate the natural frequency of the system using the following equation:

$$f_n = \frac{60}{2\pi}\sqrt{\frac{3EI}{L^3 m_{Total}}}$$

The increase in the first mode natural frequency from 21 rpm in the straight cylindrical tower to 32 rpm (0.53 Hz) in the final hybrid tower design indicates improved structural stability due to increased stiffness. Figure 15 displays the tabular data from ANSYS Workbench detailing the natural frequencies of the hybrid tower design. The hybrid design, with its tapered geometry, has a higher moment of inertia at the base compared to the straight cylinder, which enhances the overall stiffness of the structure. This additional stiffness raises the natural frequency, moving it further away from the turbine's operating frequency range and reducing the risk of resonance-induced damage.

Tabular Data

	Mode	Frequency [Hz]
1	1.	0.53409
2	2.	0.5341
3	3.	1.9694
4	4.	1.9694
5	5.	4.6033
6	6.	4.6033

Figure 15: Modes of Natural Frequency

In the FEA simulation, a point mass representing the nacelle was added, and a fixed support was applied to the bottom face of the tower to simulate its attachment to the foundation. The modal analysis was conducted to determine the natural frequency of the tower. Normal and extreme weather conditions do not affect the natural frequency, as modal analysis only considers the tower's constant mass of the nacelle and the same boundary condition. Therefore, the natural frequency remains unchanged across different loading scenarios, as external forces like wind do not influence the vibrational characteristics of the structure.

Factor of Safety against Buckling Failure:

A buckling check of the tower design is required to ensure an adequate factor of safety against buckling failure within the rigid structure. The target is to achieve a load factor of at least 8 under worst-case load conditions. The buckling load, defined as the compressive axial load at which the tower will buckle, was calculated using Euler's column formula (calculations in Appendix I):

$$P_{cr} = \frac{\pi^2 EI}{(KL)^2}$$

The applied compressive load was determined by summing the weight of the tower, nacelle, and three blades and thus the factor of safety against buckling failure was found using:

$$F.S._{buckle} = \frac{P_{cr}}{P_{applied}}$$

The factor of safety indicates that the final hybrid cylinder-tapered design can withstand loads up to 95 times greater than the critical load under extreme conditions. This factor of safety was determined through an eigenvalue buckling simulation in Ansys Workbench (Figure 16), conducted under both normal and extreme wind conditions with wind applied from behind the tower. The load multiplier, or eigenvalue buckling factor of safety, represents the factor by which the applied load must be multiplied for the structure to reach its buckling point. Thus, having a first load multiplier factor if at least 8 under worst-case (extreme weather) conditions will satisfy the required buckling constraint. The factor of safety remains the same for both extreme and normal loading conditions because the relationship between the critical load and applied compressive load remains constant.

Tabular Data

	Mode	Load Multiplier
1	1.	94.933
2	2.	95.697

Figure 16: Buckling Eigenvalues

Fatigue Analysis:

Since wind turbines face environmental stresses and high operational and maintenance costs, the fatigue life is considered. Therefore, the design needs to be stable for infinite cycles until failure. Fatigue analysis was conducted using an experimental S-N curve, which provides a relationship between cyclic stress amplitude and the number of cycles to failure. This curve, drawn from existing literature, allows for the estimation of fatigue life based on repetitive loading conditions typical of wind turbine operation. The fatigue analysis assumes that the material remains within its elastic range throughout its service life, allowing the use of a stress-life approach without the need to account for plastic deformation; this choice is practical for wind turbine structures, which are generally designed to avoid stresses that exceed the elastic limits of their materials. On the experimental S-N curve, stainless steel is shown to have a fatigue limit of 39 ksi. This means that after infinite elastic cycles stainless steel can still safely handle stresses up to 39 ksi (but not necessarily the yield stress of 42 ksi). All steel components of the design are modeled as having a maximum strength of 39 ksi to account for fatigue.

Analysis of Baseplate Connection

The bolted flange connection was designed to provide stability for the wind turbine by resisting forces and moments acting on the tower. Key design steps included calculating the required base plate thickness, determining the appropriate bolt type and number, and verifying that the selected bolts could withstand the stresses and loading of the tower. A factor of safety of 6 was applied so that the hardware could support the tower's loading.

The 36-inch-thick base plate is flanged and anchored to a concrete foundation using B7M bolts manufactured by Lightning Bolt Supply. The flange design includes 75 bolts, each with a 7-inch diameter and a yield strength of 100 ksi. The number of bolts was determined by shear and tensile stress calculations, with a max allowable shear of 6.3 ksi, and max allowable tensile stress 16.7 ksi (detailed calculations in Appendix I). The shear stress across all the bolts was determined to be 0.4 ksi < 6.3 ksi. The maximum tensile stress in any bolt in the pattern in the worst-case scenario was determined to be 14.9 ksi < 16.7 ksi. The number of bolts were chosen to satisfy the tensile stress calculation.

To accurately model the flange and baseplate, the tower and flange were initially combined as a single body. As previously noted, this required using a tetrahedral mesh due to the filleted region of the flange. The mesh became very coarse around the fillet and bolt holes, which would lead to inaccuracies in stress and deformation analysis. However, the tower maintained a relatively fine mesh above the filleted area, indicating that node displacements in that region were still accurate.

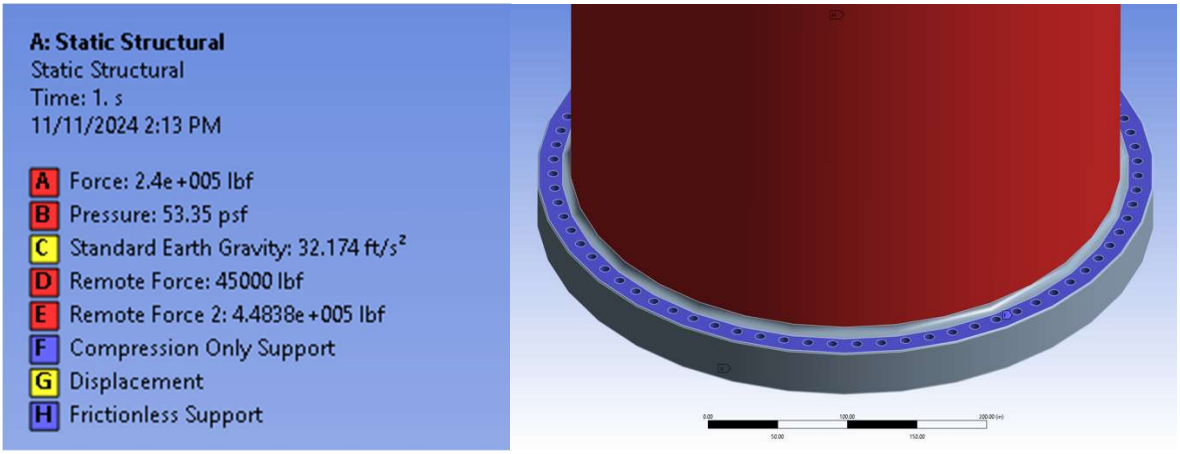

Figure 17: Constraints of Large Reference Model

A simplification was made in the model: instead of including 75 individual washers with compression constraints applied to each one, a single compression constraint was placed on the top of the baseplate, omitting the washers. While this approach increases the effective compressed area, it was chosen to avoid the coarse mesh that would result from modeling each washer individually. Initially, the washers were modeled, but they were ultimately excluded for this reason.

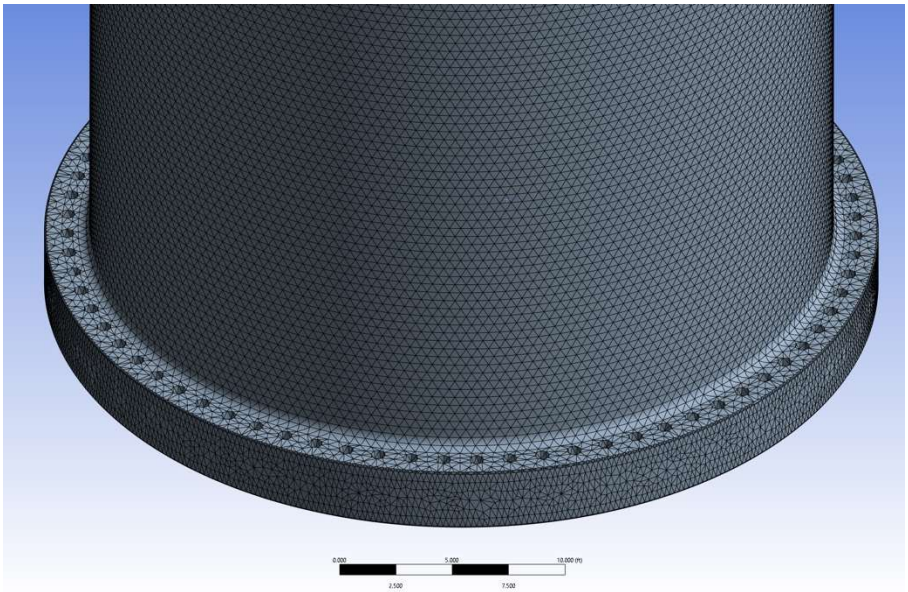

Figure 18: Mesh of Large Reference Model

To enhance accuracy around the baseplate, two sub-models were generated using the slice feature in Design Modeler: one focusing on the bolt hole ring and the other on a segment of the ring. Notably, the sub models could not be meshed using the multizone hexa/prism method. To address this, a tetrahedral mesh with an element size of 2 inches was used for the ring and an element size of 0.5 inches was used for the segment of the ring, enabling the generation of accurate results. Inflation around the holes of the ring sub model (settings: 0.5 growth rate, 2 layers, 0.5 transition ratio) was used to provide fine circular elements around the bolt holes. The baseplate flange mesh is displayed in Figures 19 and 20.

Figure 19: Slice with Tetrahedral Mesh of Baseplate

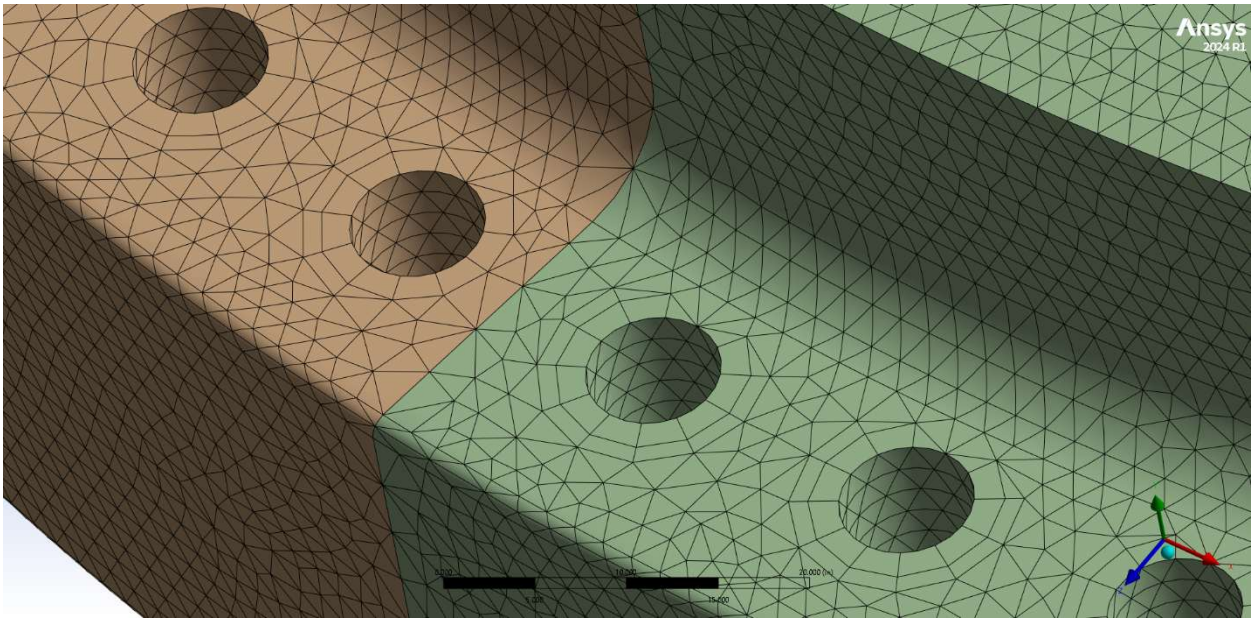

Figure 20: Slice with Tetrahedral Mesh of Baseplate (Zoomed-In)

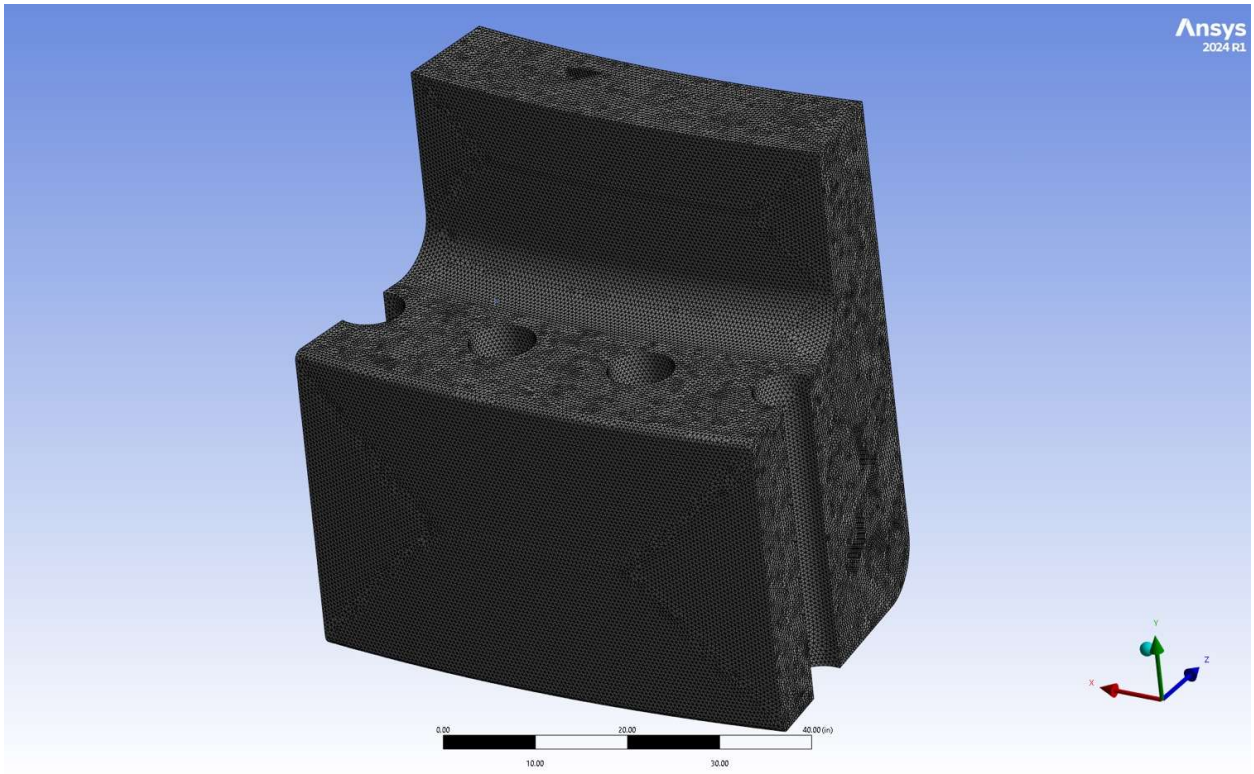

Figure 21: Slice with Tetrahedral Mesh of Baseplate Segment

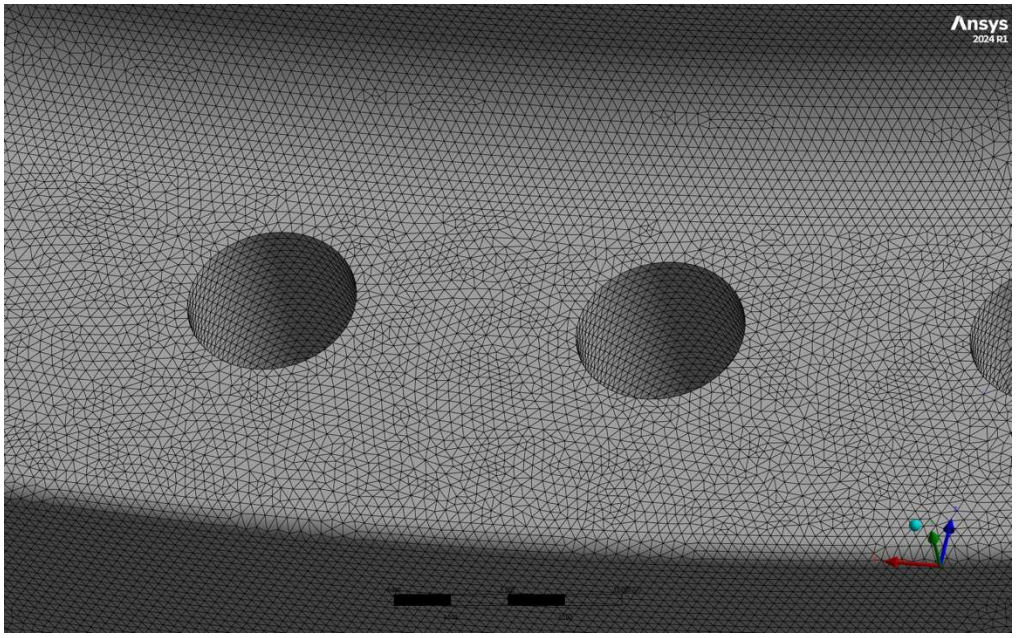

Figure 22: Slice with Tetrahedral Mesh of Baseplate Segment (Zoomed-In)

These sliced geometries were treated as a separate ‘Static Structural’ block in Workbench, where solution information from the single-body model was transferred to the setups of the sliced geometries. This enabled the ‘sub-modeling’ menu in the setup, which required the addition of constraints. A cut boundary constraint was applied to all faces on the sliced piece that connects to the larger single-body model, allowing nodal displacements from the large model to transfer appropriately to the corresponding faces in the sub-model (shown in Figures 23 and 24). The advantage of this approach is that the bolt holes in the sub-model can be meshed much more finely than in the full model, resulting in more accurate stress and deformation results. It’s worth noting that the sub-model doesn’t require additional constraints, as those from the larger model are carried over. Sub-modeling provides the benefit of obtaining highly accurate results in a specific region of a larger structure, as long as nodal displacements are accurately tracked from the large model.

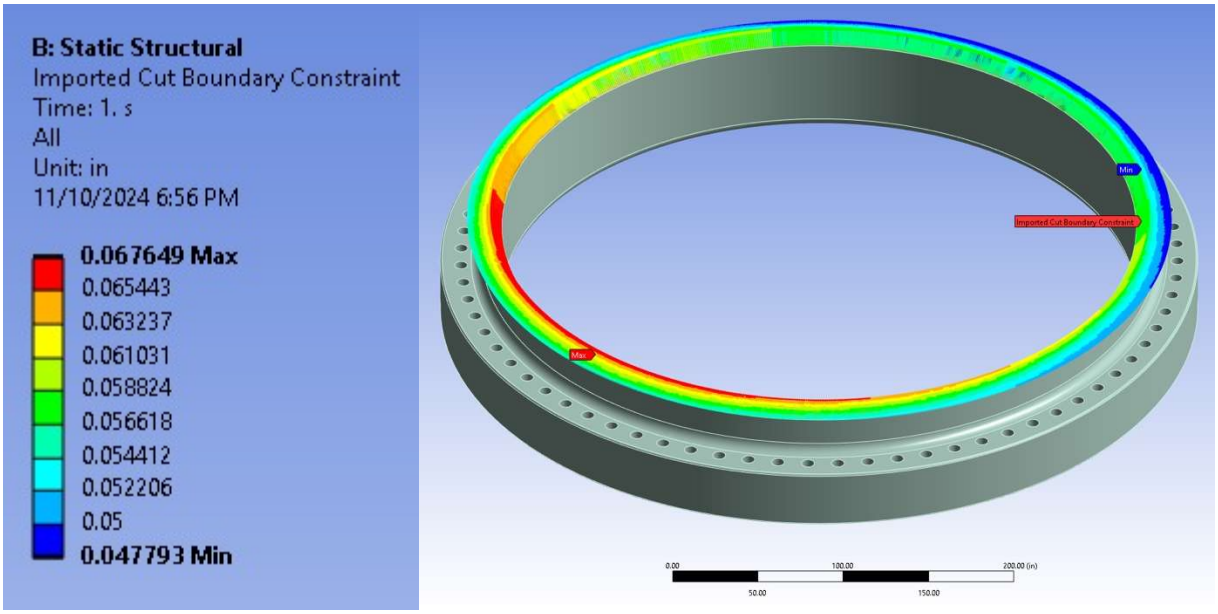

Figure 23: Nodal Displacement Vectors of Baseplate

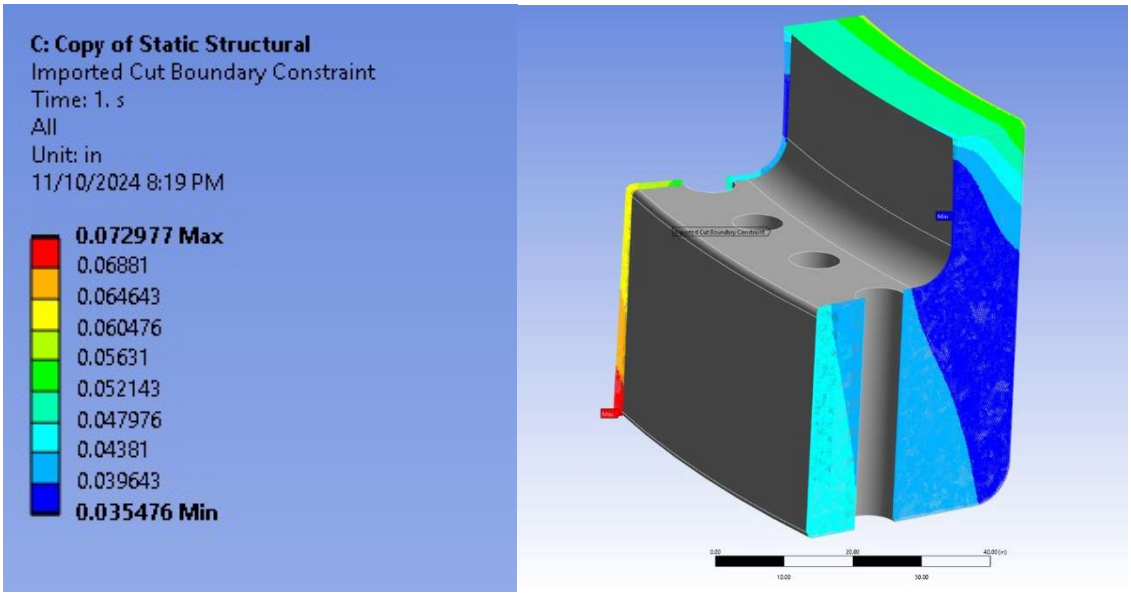

Figure 24: Slice with Nodal Displacement Vectors of Baseplate Segment

In the initial iteration, a 12-inch-thick base plate met the maximum allowable stress limit of 23.7 Ksi at ambient (62.5°F) and extreme cold (-10°F) temperatures under both normal and extreme wind conditions. However, this thickness was insufficient for the extreme hot temperature (135°F), where stresses of 50 ksi were observed near the bolt holes. To address this, the base plate thickness was increased to 36 inches. This adjustment ensured that the stress criterion of 23.7 ksi was met across all temperature scenarios, as shown in the images below, confirming that the base flange remains within safe stress limits and meets the required material safety factor of 1.65. Notably, the stress color bar scales were adjusted in each temperature case by probing stresses at the bolt holes and setting the maximum values on the bars to be 5,000-10,000 psi higher than the recorded values. This approach enables a visible stress gradient to be displayed along the bolt holes.

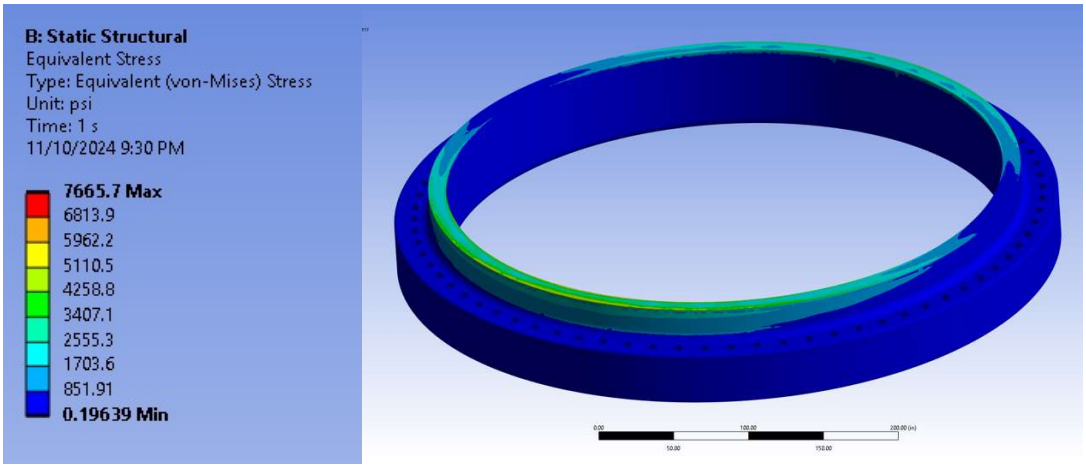

Figure 25: Maximum Von Mises Stress of Baseplate Under -10°F

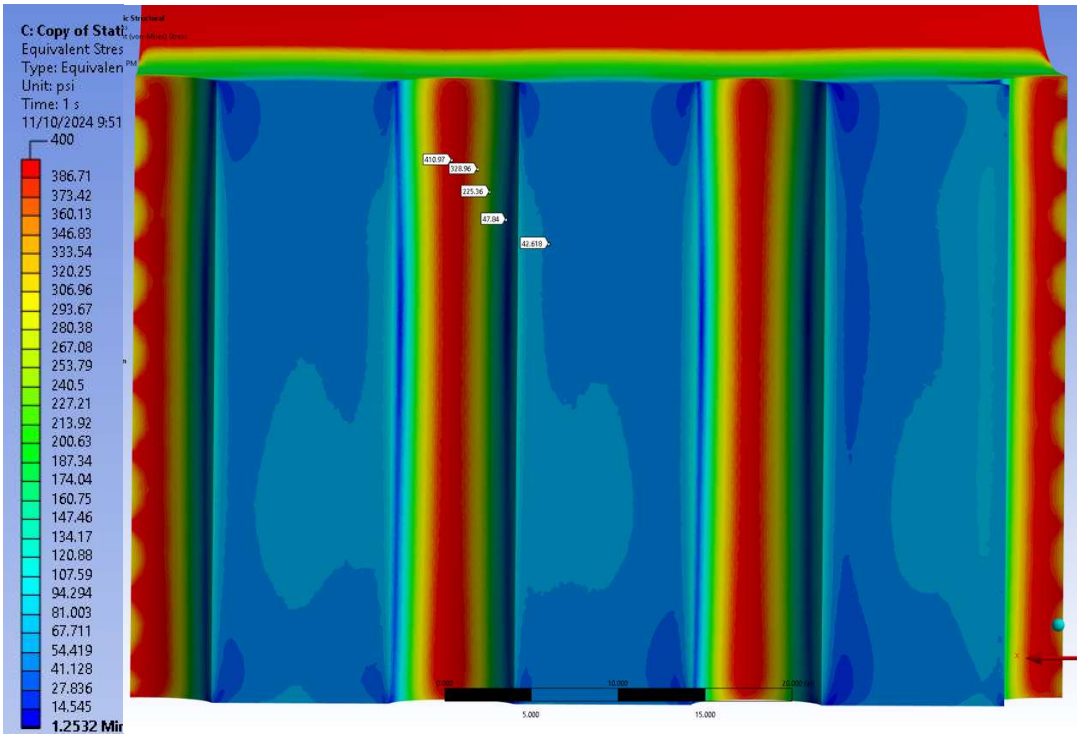

Figure 26: Maximum Von Mises Stress of Baseplate Compression Segment Under -10°F

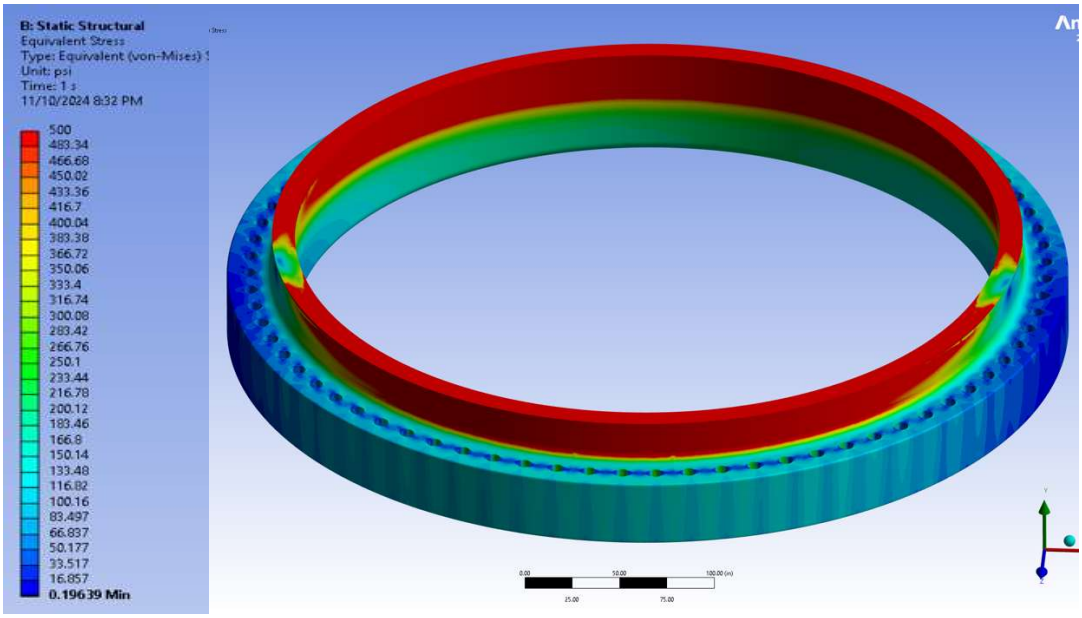

Figure 27: Maximum Von Mises Stress of Baseplate Under 62.5°F

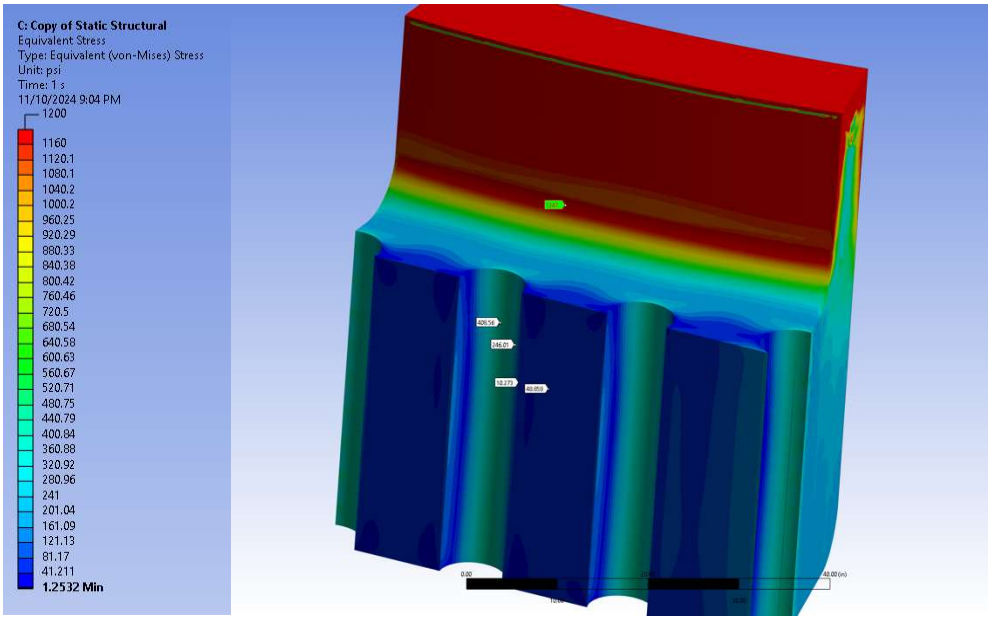

Figure 28: Maximum Von Mises Stress of Baseplate Compression Segment Under 62.5°F

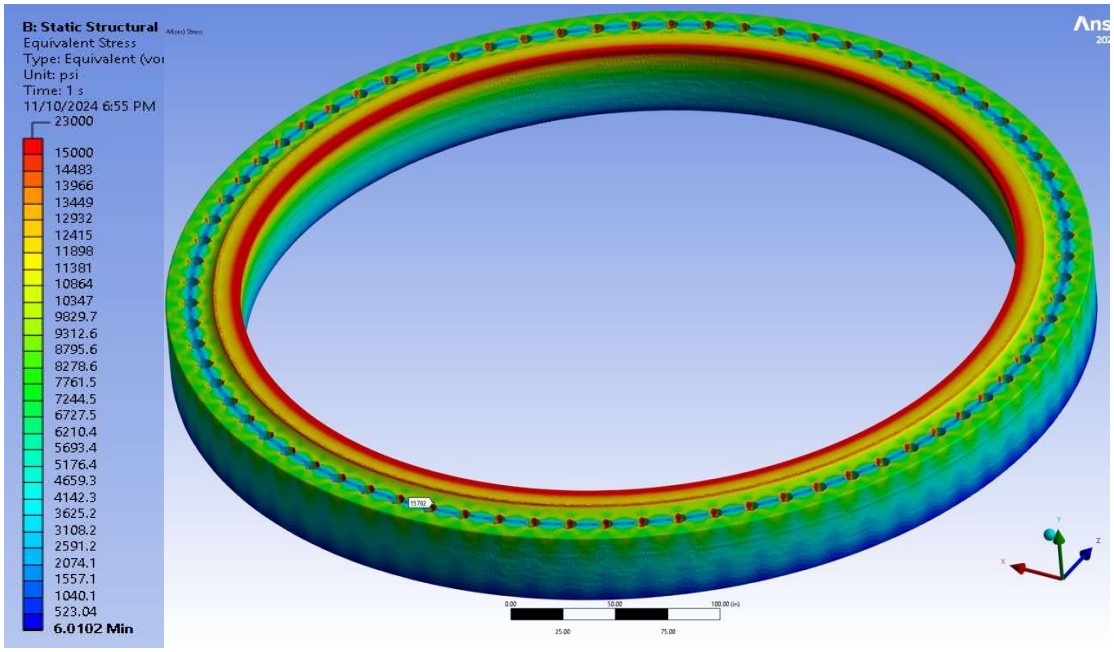

Figure 29: Maximum Von Mises Stress of Baseplate Under 135°F

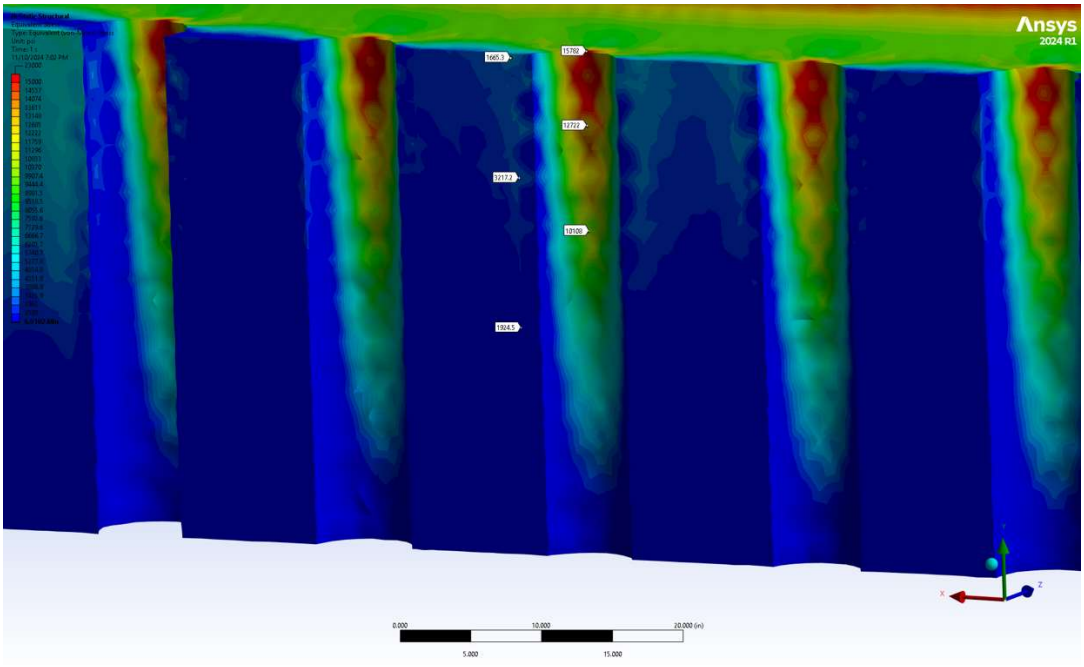

Figure 30: Maximum Von Mises Stress of Baseplate Compression Segment Under 135°F

Design Methodology to Allow Thermal Movement in Baseplate

Due to the temperature ranges of -10°F to 135°F, the baseplate flange body could undergo thermal expansion and contraction. The design methodology to accommodate this thermal movement in the base flange, was to incorporate tolerancing to ensure that the B7M bolts could effectively hold down the baseplate, despite contraction and expansion of bolt holes. Three temperature cases were analyzed for thermal movement to see which temperature (-10°F, 62.5°F, 135°F) causes the most deformation; it was found that the greatest change in radius ΔR due to any given change in temperature Δ°F was 0.3 in (details in Appendix I). As such, the maximum deformation values around the holes were the minimum tolerancing used for the bolt holes, and the bolt holes were modeled as having a diameter of 7.6 in to accommodate this.

Conclusion:

The final design of the wind turbine tower was optimized to minimize cross-sectional area and mass while satisfying specific performance and safety requirements. Finite element analysis, supported by hand calculations and meshing analysis, confirmed the tower's compliance with all stipulated regulations. The design avoids overengineering, as the cross-section was calibrated to allow for deflection under extreme weather conditions just within the permissible range. Additionally, the bolted flange was adjusted to remain just below the specified stress safety factor at the steel's fatigue limit.

APPENDICES

Design time estimate: 20 hours
Cumulative hours spent developing design: 160 hours

Appendix I – Hand Calculations

Note: N subscript indicates normal conditions, and EX indicates extreme weather conditions

Table 10: Parameters Used in Basic Hand Calculations

Parameters	Symbol	Value	Units
Height of Tower	L	525	ft
Coefficient of Drag of Blades	C_d	0.8	-
Coefficient of Drag of Tower	$C_{d\,(t)}$	1.1	-
Outer Diameter of Tower	$w_{(t)}$	36	ft
Air Density	ρ_{air}	0.07967	lbm/ft^4

Maximum Allowable Stress Due to Fatigue

$$\sigma_{all} = \frac{\sigma_{yield}}{FS} = \frac{39160\ psi}{1.65} = \mathbf{23733\ psi}$$

Force caused by wind on blades:

$$P_x = P_{blades}\,A = \frac{C_d \rho_{air} v^2}{2}\ 3 w_b l_b$$

$$P_{x\,N} = \frac{0.8\left(0.07967\,\frac{lb_m}{ft^3}\right)\left(102.667\ \frac{ft}{s}\right)^2}{2\left(32.2\ \frac{lb_m}{slug}\right)}\ 3(215\ ft)(17.9\ ft) = \mathbf{120,560\ lb_f}$$

$$P_{x\,EX} = \frac{0.8\left(0.07967\,\frac{lb_m}{ft^3}\right)\left(198\ \frac{ft}{s}\right)^2}{2\left(32.2\,\frac{lb_m}{slug}\right)}\ 3(215\ ft)(17.9\ \ ft) = \ \mathbf{448,380\ lb_f}$$

Moment caused by weight of blades:

$$M_y = W_{blades}(\text{offset}) = 3\left(15000\ lb_f\right)(32ft) = \mathbf{1.44\ \times 10^6\ lb_f \cdot ft}$$

Pressure caused by wind on tower:

$$w_x = \frac{C_d \rho V^2}{2} w_{(t)}$$

$$P_{tower} = \frac{C_d \rho V^2}{2} = \frac{1.1\left(0.07967 \frac{lbm}{ft^3}\right)\left(198 \frac{ft}{s}\right)^2}{2\left(32.2 \frac{lb_m}{slug}\right)} = 53.34 \frac{lbf}{ft^2}$$

$$w_{x\,N} = \frac{C_{d\,(t)}\left(0.07967 \frac{lb_m}{ft^3}\right)\left(102.667\ {}^{ft}/_{s}\right)^2}{2\left(32.2 \frac{lb_m}{slug}\right)} w_{(t)} = \mathbf{13.04}\ \frac{\boldsymbol{lbf}}{\boldsymbol{ft^2}} \cdot\ \boldsymbol{C_{d\,(t)} w_{(t)}}$$

$$w_{x\,EX} = \frac{C_{d\,(t)}\left(0.07967 \frac{lbm}{ft^3}\right)\left(198 \frac{ft}{s}\right)^2}{2\left(32.2 \frac{lb_m}{slug}\right)} w_{(t)} = \mathbf{48.50}\ \frac{\boldsymbol{lbf}}{\boldsymbol{ft^2}} \cdot\ \boldsymbol{C_{d\,(t)} w_{(t)}}$$

Maximum Deflection:

$$\delta_{max} = \delta_{wind,t} + \delta_{wind,b} + \delta_{moment,b}$$

$$\delta_{max} = \frac{M_y L^2}{2EI} + \frac{P_x L^3}{3EI} + \frac{w_x L^4}{8EI}$$

$$\delta_{max} = \frac{8P_x L^3 + 3w_x L^4 + 12M_y L^2}{24EI}$$

To perform hand calculations for structural analyses, the moment of inertia I was determined based on the requirement that deflection under extreme conditions should not exceed L/370. The inequality used to solve for I is as follows:

$$I > 370 \frac{8P_x L^2 + 3w_x L^3 + 12M_y L}{24E}$$

where $E = 29 \times 10^6\ psi = 4.032 \times 10^9\ psf$.

Given the parameters of $C_{d\,(t)}$ and $w_{(t)}$ (values given in Table 99), and the use of a hollow cylindrical shape, it is found that I > 7103 ft^4 and tower thickness of around 32 ft.

Based on this requirement, an initial design iteration of a hollow cylindrical tower with an outer diameter of 36 ft and an inner diameter of 35 ft was selected for both the first basic simulations

and hand calculations. This configuration gives a moment of inertia of I = 8786 ft^4, which satisfies the inequality for the required moment of inertia under extreme conditions (which is expected to cause greatest tower deflection).

$$\delta_{\max N} = \frac{8(P_{x\,N})L^3 + 3(w_{x\,N})L^4 + 12\left(M_{y\,N}\right)L^2}{24EI} < \frac{L}{500}$$

$$\frac{8\left(120{,}560\ lb_f\right)(525\ ft)^2 + 3(1.1)\left(13.04\ \frac{lbf}{ft^2}\right)(36\ ft)(525\ ft)^3 + 12(1.44\ \times 10^6\ lbf \cdot ft)(525\ ft)}{24\left(4{,}032{,}000{,}000\ \frac{lbf}{ft^2}\right)(8786\ ft^4)} < \frac{525ft}{500}$$

$\delta_{\max N} = \mathbf{0.31\ ft} < 1.05$ ft

$$\delta_{\max EX} = \frac{8(P_{x\,EX})L^2 + 3(w_{x\,EX})L^4 + 12\left(M_{y\,EX}\right)L^2}{24EI} < \frac{L}{370}$$

$$\frac{8\left(448{,}380\ lb_f\right)(525\ ft)^2 + 3(1.1)\left(48.50\ \frac{lbf}{ft^2}\right)(36\ ft)(525\ ft)^3 + 12(1.44\ \times 10^6\ lbf \cdot ft)(525\ ft)}{24\left(4{,}032{,}000{,}000\ \frac{lbf}{ft^2}\right)(8786\ ft^4)} < \frac{525ft}{370}$$

$\delta_{\max EX} = \mathbf{1.13\ ft} < 1.42$ ft

The maximum deflections of the normal and extreme weather conditions are shown to be less than the deflection limits in the design specifications.

<u>Maximum Stress: Normal Conditions</u>

$Q_{max} = P_x + w_x L$ (internal shear stress located at base of tower)

$$Q_{max\,N} = P_{x\,N} + w_{x\,N}L = 120{,}560\ lb_f + \left(13.04\ \frac{lb_f}{ft^2} \cdot\ C_{d\ (t)}w_{(t)}\right)(525ft)$$

$$= 120{,}560\ lb_f + \left(13.04\ \frac{lb_f}{ft^2} \cdot 1.1 \cdot 36ft\right)(525ft) = 391662\ lb_f$$

$$\tau_{max\,N} = \frac{Q_{max\,N}}{A} = \frac{391662\ lb_f}{\frac{\pi}{4}[(36\ ft)^2 - (35\ ft)^2]} = 7024\ psf = 49\ psi$$

$M_{max} = M_y + P_x L + \frac{w_x L^2}{2}$ (located at base of tower)

$$M_{\max N} = M_y + P_{x\,N} L + \frac{w_{x\,N} L^2}{2}$$
$$= 1.44 \times 10^6\ lb_f \cdot ft + (120{,}560\ lb_f)(525 ft)$$
$$+ \frac{\left(13.04\ \frac{lb_f}{ft^2} \cdot 1.1 \cdot 36 ft\right)(525 ft)^2}{2} = 135898170\ lb_f \cdot ft$$

$$\sigma_{max} = \sigma_{bending} + \sigma_{axial} = \frac{M_{max}\left(\frac{h}{2}\right)}{I} + \frac{P}{A}$$

$$\sigma_{max\,N} = \frac{M_{max}\left(\frac{h}{2}\right)}{I} + \frac{W_{nacelle} + W_{blades}}{A}$$
$$= \frac{(135898170\ lb_f \cdot ft)\left(\frac{36ft}{2}\right)}{8786\ ft^4} + \frac{240000 lb_f + 3(15000 lb_f)}{\frac{\pi}{4}[(36\ ft)^2 - (35\ ft)^2]}$$
$$= \mathbf{284{,}930\ psf = 1979\ psi}$$

Maximum Stress: Extreme Conditions

$$Q_{max\,EX} = P_{x\,EX} + w_{x\,EX} L = 448{,}380\ lb_f + \left(48.50\ \frac{lb_f}{ft^2} \cdot\ C_{d\,(t)} w_{(t)}\right)(525 ft)$$
$$= 448{,}380\ lb_f + \left(48.50\ \frac{lb_f}{ft^2} \cdot 1.1 \cdot 36 ft\right)(525 ft) = 1456695\ lb_f$$

$$\tau_{max\,EX} = \frac{Q_{max\,EX}}{A} = \frac{1456695\ lb_f}{\frac{\pi}{4}[(36\ ft)^2 - (35.5\ ft)^2]} = 26{,}123\ psf = 181\ psi$$

$$M_{\max EX} = M_y + P_{x\,EX}L + \frac{w_{x\,EX}L^2}{2}$$
$$= 1.44 \times 10^6\ lb_f \cdot ft + (448{,}380\ lb_f)(525ft)$$
$$+ \frac{\left(48.50\ \frac{lb_f}{ft^2} \cdot 1.1 \cdot 36ft\right)(525ft)^2}{2} = 501522188\ lb_f \cdot ft$$

$$\sigma_{max} = \sigma_{bending} + \sigma_{axial} = \frac{M_{max}\left(\frac{h}{2}\right)}{I} + \frac{P}{A}$$

$$\sigma_{max\,EX} = \frac{M_{max}\left(\frac{h}{2}\right)}{I} + \frac{W_{nacelle} + W_{blades}}{A}$$
$$= \frac{(501522187\ lb_f \cdot ft)\left(\frac{36ft}{2}\right)}{8786\ ft^4} + \frac{240000lb_f + 3(15000lb_f)}{\frac{\pi}{4}[(36\ ft)^2 - (35\ ft)^2]}$$
$$= \mathbf{1{,}032{,}586\ psf = 7171\ psi}$$

The normal σ and shear τ stresses of the tower under normal and extreme conditions were found and are both less than the maximum allowable yield stress under strength safety factor of 1.65.

Thermal Effects: Tower Height Change

For 135°F:

$$\Delta L = \alpha(T_H - T_0)L = \left(9.61 \times 10^{-6}\ \frac{in}{in°\text{F}}\right)(135°\text{F} - 62.5°\text{F})\,(525\ ft)\left(\frac{12\ in}{1\ ft}\right) = \mathbf{4.39\ in}$$

For -10°F:

$$\Delta L = \alpha(T_0 - T_C)L = \left(9.61 \times 10^{-6}\ \frac{in}{in°\text{F}}\right)\big(62.5°\text{F} - (-10°\text{F})\big)(525\ ft)\left(\frac{12\ in}{1\ ft}\right) = \mathbf{-4.39\ in}$$

Thermal Effects: Flange Radius Change

For 135°F:

$$\Delta R = \alpha(T_0 - T_C)R = \left(9.61 \times 10^{-6}\ \frac{in}{in°\text{F}}\right)\big(135°\text{F} - (62.5°\text{F})\big)(37\ ft)\left(\frac{12\ in}{1\ ft}\right) = \mathbf{0.3\ in}$$

For -10°F:

$$\Delta R = \alpha(T_0 - T_C)L = \left(9.61 \times 10^{-6}\ \frac{in}{in°\text{F}}\right)\big(62.5°\text{F} - (-10°\text{F})\big)(37ft)\left(\frac{12\ in}{1\ ft}\right) = \mathbf{-0.3\ in}$$

Shear Force on Bolts

$P_{x\,EX} = 448{,}380\ lb_f$

$P_{tower} * XS_{tower} = 53.34\ \frac{lbf}{ft^2} * 12731.25\ ft^2 = 679208\ lbf$

$V_{max} = P_{x\,EX} + P_{tower} * XS_{tower} = 1127588\ lbf$

The total shear across all bolts is $\tau_{bolts} = \frac{V_{max}}{(cross\ sectional\ area\ of\ all\ bolts\ combined)}$

Given that a 7-inch diameter bolts is used, in an equally spaced bolt pattern of 75 bolts, the total cross-sectional area of all bolts combined is:

$XS_{total} = \pi(3.5in)^2 * 75 = 2886\ in^2$

Thus, the total shear across all bolts is:

$$\tau_{bolts} = \frac{1127588\ lbf}{2886\ in^2} = \mathbf{391\ psi}$$

The maximum tensile strength of B7M bolts is 100 ksi. Given that $\tau_{yield} \approx \frac{1}{2}\sigma_{yield}$ under Tresca Criterion, the maximum shear strength is 50 ksi. Applying the factor of safety of 6 on all connecting components, the maximum allowable shear is $\frac{\tau_{yield}}{6} = \mathbf{8.3\ ksi}$

Tensile Stress on Bolts Due to Total Moment

The maximum tensile strength of B7M bolts is 100 ksi, thus the maximum allowable stress is

$$\sigma_{all} = \frac{\sigma_{yield}}{6} = 16.7\ ksi$$

The Python script to find maximum tensile stress in any given bolt is shown in Figure 29.

The Maximum Tensile Stress found by the Python Code is **14.9 Ksi < 16.7 Ksi**, satisfying the maximum allowable tensile stress condition.

```python
import numpy as np

r_boltpattern = 17.5  # Radius of Bolt Circle
r_bolt = 7/24         # Radius of bolt (7 inches converted to ft)
num_bolt = 75         # Number of bolts
M_tot = 479463959     # Total moment lbf-ft
# Number of bolts
a_bolt = np.pi * r_bolt ** 2  # Cross-sectional area of a bolt (ft^2)

angles = np.linspace(0, 2*np.pi, num_bolt, endpoint=False) # Define angles
perp_distances = r_boltpattern * np.sin(angles)            # Define perpendicular Distances using sin
total_capacity = np.sum(np.abs(perp_distances))            # Sum of all Perpendicular Distances
max_tensile_stress = 0                                     # Initialize array

for j, d_p in enumerate(perp_distances):                   # For Loop
    if abs(d_p) < 1e-7:                                    # Error when d_p < 0, so set to a very small value
        continue
    moment_share = (abs(d_p) / total_capacity) * M_tot     # Moment Share of each bolt in for loop (lbf-ft)
    tensile_force = moment_share / abs(d_p)                # Tensile Force from the Moment Share in any given bolt
    tensile_stress = tensile_force / a_bolt                # Stress from tensile force
    if tensile_stress > max_tensile_stress:                # Replace value of tensile force if > Last
        max_tensile_stress = tensile_stress                # Stress in Psf

print(max_tensile_stress/144)                              # Print Final Value in Psi
```

Figure 29: Code to Calculate the Maximum Tensile Stress in Any Given Bolt

Natural Frequency: Blade Failure

The tower was treated as a cantilever beam with a load at the free and the natural frequency of the tower, f_n , was calculated using the formula:

$$f_n = \frac{1}{2\pi}\sqrt{\frac{k}{m_{Total}}}$$

where k is the stiffness of a cantilever beam, given by:

$$k = \frac{3EI}{L^3}$$

and m_{Total} is the effective mass at the free end of the wind turbine, approximated as:

$$m_{Total} \approx m_{nacelle} + 0.23m_{tower}$$

The weight of the blades was neglected, as explained in the results section. The effective mass of the tower was calculated as:

$$m_{tower} = \frac{W_{tower}}{g} = \frac{24882\ lb_f}{32.2\frac{ft}{s^2}}\left(\frac{32.2\frac{lb_m ft}{s^2}}{1lb_f}\right) = 27324\ lb_m$$

To express the natural frequency in RPM, the formula becomes:

$$\omega_n = \frac{60}{2\pi}\sqrt{\frac{3EI}{L^3 m_{Total}}} = \frac{60}{2\pi}\sqrt{\frac{3(4.032\ \times\ 10^9\ psf)(8786\ ft^4)}{(525\ ft)^3(240000lb_m + 27324\ lb_m)}} = \mathbf{21\ RPM}$$

Buckling Check

The maximum critical buckling load, defined as the compressive load at which the tower will buckle, was calculated using Euler's column formula:

$$P_{cr} = \frac{\pi^2 EI}{(KL)^2}$$

where K = 2 as the tower (treated as a cantilever beam) since is fixed at one end and free at the other. Substituting in values:

$$P_{cr} = \frac{\pi^2(4.032 \times 10^9\ psf)(8786\ ft^4)}{(2 * 525ft)^2}$$

Assuming the applied load is the total weight (consisting of the nacelle, blades, and tower) and that the cross-section of the column is uniform throughout its length. The factor of safety against buckling is calculated as:

$$F.S._{buckling} \leq \frac{P_{cr}}{applied\ load} = \frac{P_{cr}}{W_{nacelle} + 3W_{blades} + W_{tower}}$$

The weight of the tower is calculated below:

$$W_{tower} = \rho gAL = \left(490\frac{lb_m}{ft^3}\right)\left(\frac{1lb_f}{32.2\frac{lb_m ft}{s^2}}\right)\left(32.2\frac{ft}{s^2}\right)\left(\frac{\pi}{4}[(36\ ft)^2 - (35\ ft)^2]\right)(525ft)$$

$$= 27324\ lb_f$$

Since the tower must withstand a factor of safety of 8 under all loading conditions:

$$8 \leq \frac{P_{cr}}{240000lb_f + 3(15000lb_f) + 27324lb_f} = \mathbf{31}$$

The inequality is satisfied, indicating that the buckling condition is met with a sufficient factor of safety.

Desmos Optimization

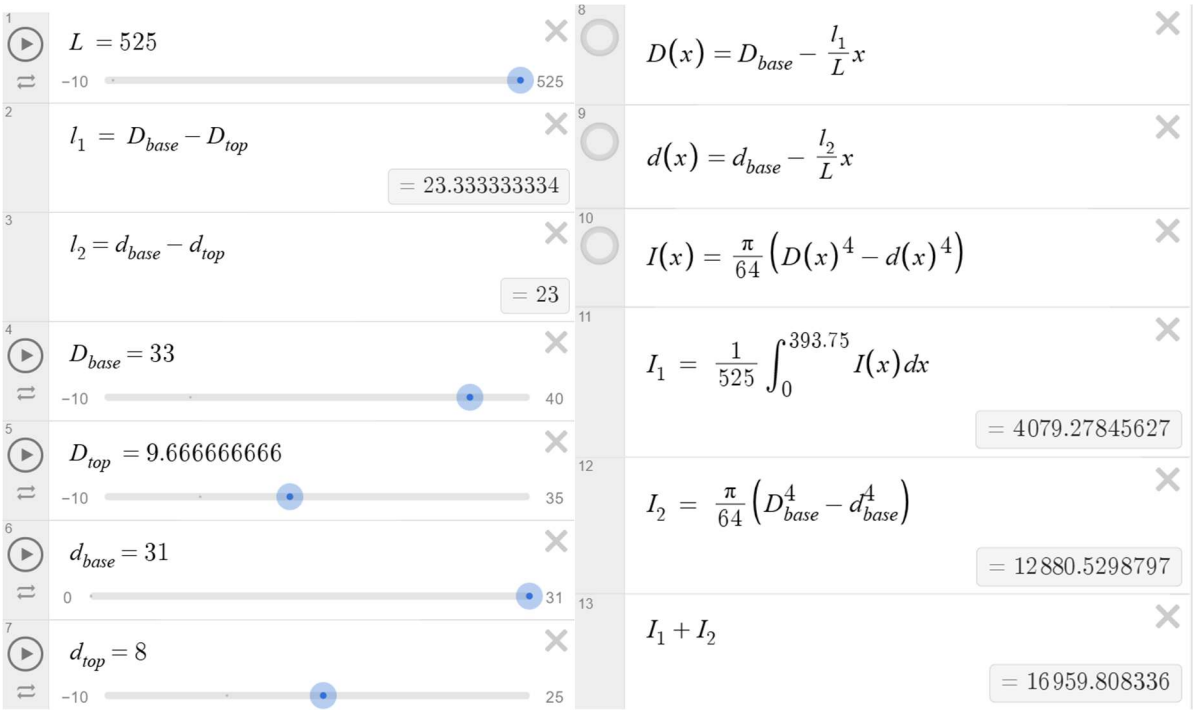

Desmos To find I

Appendix II – Additional Mesh Analysis

The mesh used for the tower deemed satisfactory on account of the solution results were unaffected by increasing the quality of the mesh. This was determined by comparing the solution from the initial mesh of the tower (Workbench's default sized automatic method mesh) with the solution from the final mesh of the tower (Patch conforming 1-foot sized tetra mesh)

	Initial Mesh	**Final Mesh**
Equivalent Stress (Normal)	2.86 ksi	2.85 ksi
Equivalent Stress (Extreme*)	6.60 ksi	6.62 ksi
Deflection (Normal)	0.305 ft	0.306 ft
Deflection (Extreme*)	1.100 ft	1.101 ft
Natural Frequency	0.63502 Hz	0.6502 Hz

Based on the discrepancies in results lying in insignificant figures, it was determined that the mesh was adequate.

Appendix III – Additional Simulation Analysis Images

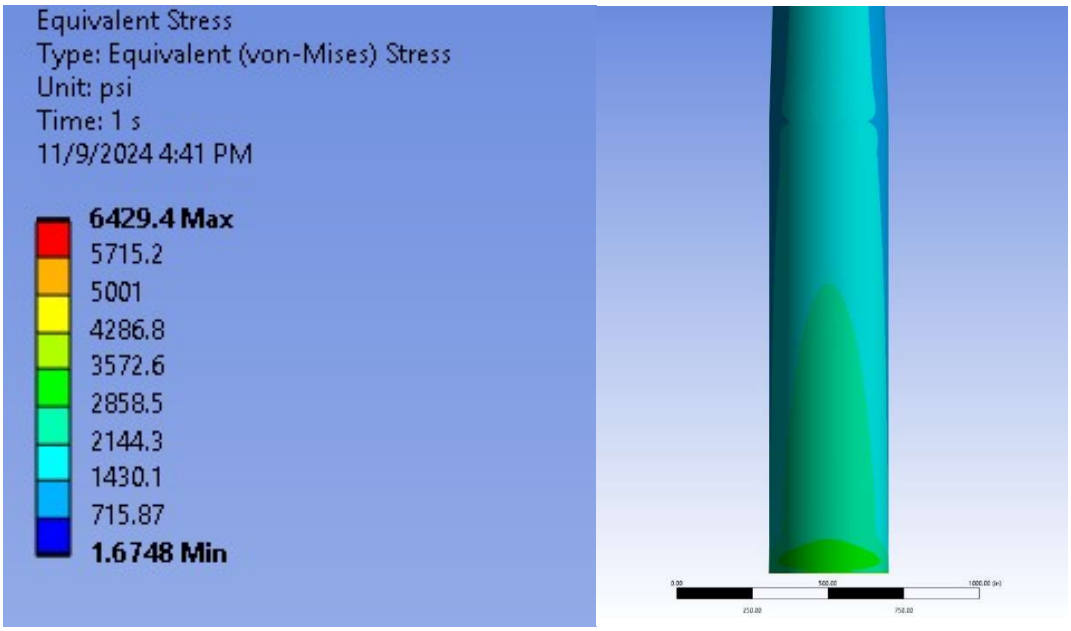

Von Mises Stress under Normal Conditions (Compressive Side) at 62.5°F

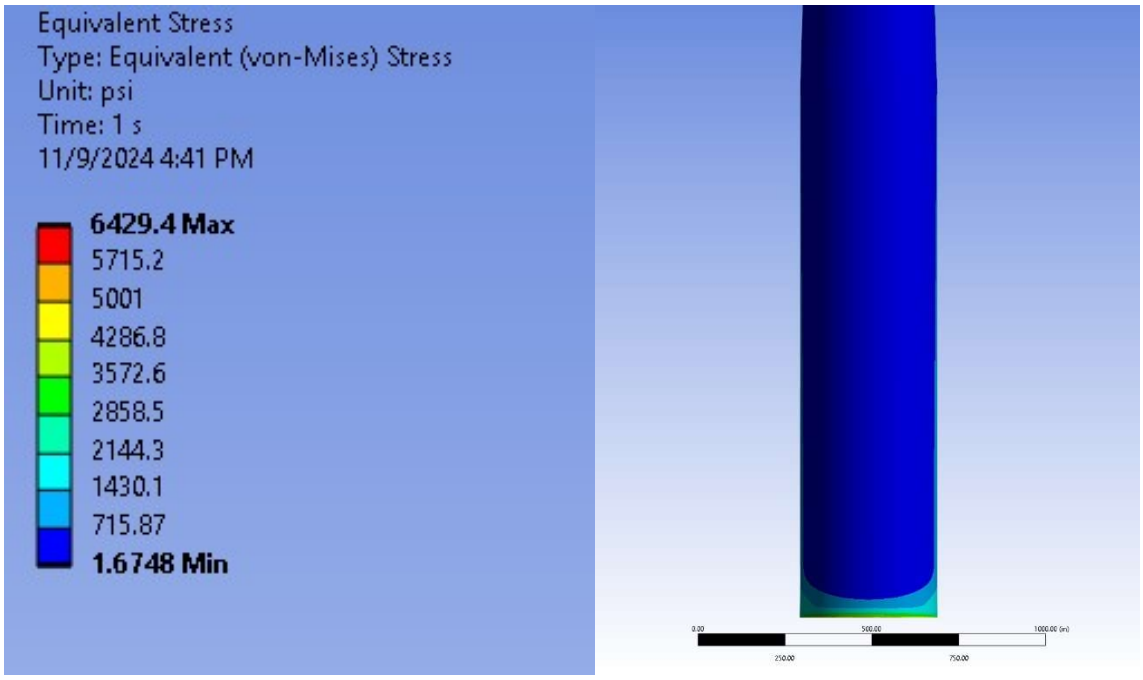

Von Mises Stress under Normal Conditions (Tensile Side) at 62.5°F

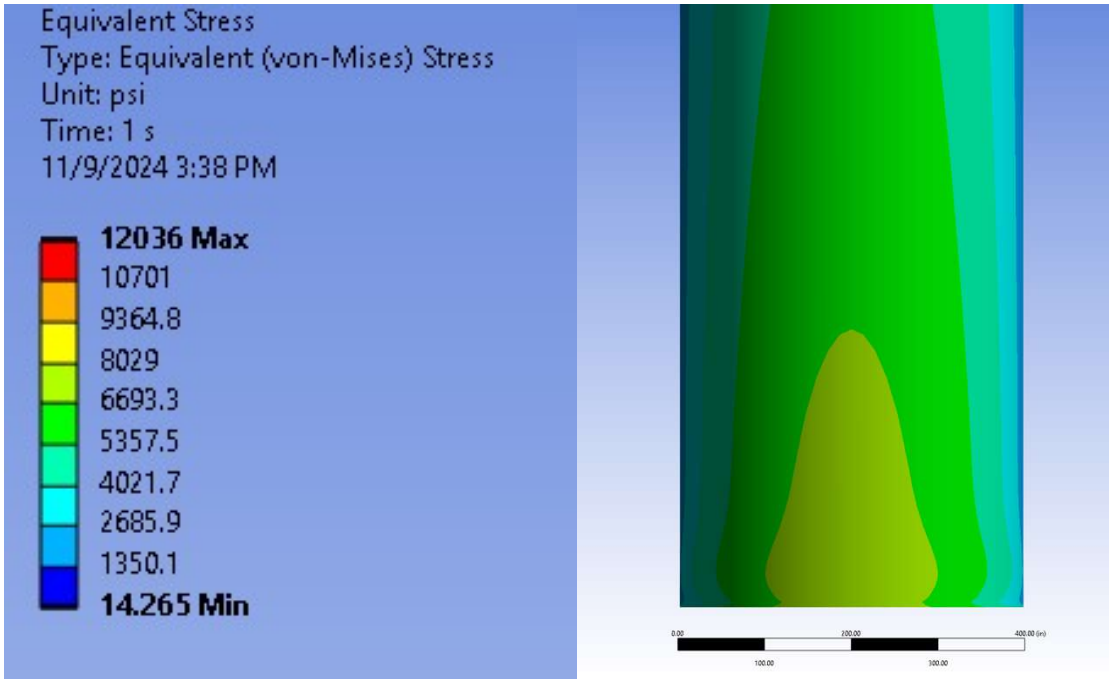

Von Mises Stress under Extreme Conditions (Compressive Side) at 62.5°F

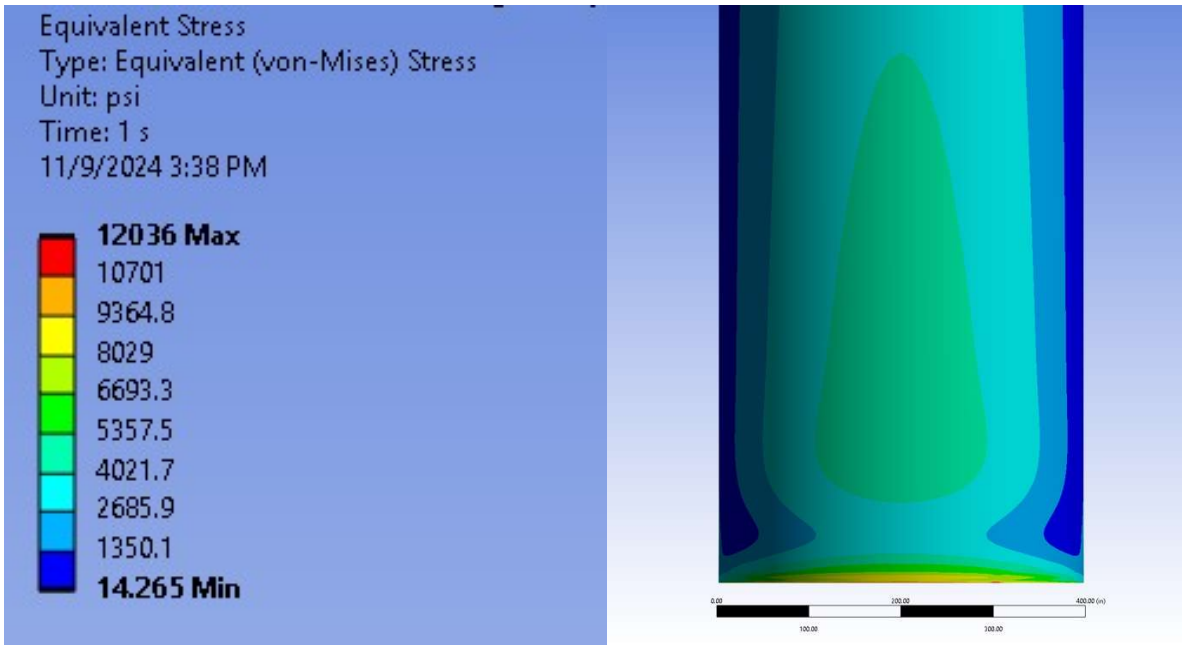

Von Mises Stress under Extreme Conditions (Tensile Side) at 62.5°F

Appendix IV – Data Sourcing

Bolt Sourcing

The bolts sourced are from Lightning Bolt Supply, based out of Baton Rouge, Louisiana. They are B7M Chromium - Molybdenum bolts.

Table 11: Specifications of B7M bolts

Diameter (in)	Tensile Strength Minimum [ksi]	Hardness Max Brinell	Hardness Max Rockwell
7	100	235	B99

The link to the bolts is attached:
https://lightningboltandsupply.com/astm-a193-b7m-stud-bolts.html

Fatigue Data

The Fatigue data was sourced from the British Stainless-Steel Association. They classify Stainless Steel AISI 316 as having an endurance limit of 270 MPa. They define an endurance limit (also known as fatigue limit) as the stress level where failure does not occur after 10^6 (1 million) or 10^7 (10 million) cycles. 270 MPa is approximately **39 Ksi.**

The link about the fatigue limit is attached:
https://bssa.org.uk/bssa_articles/fatigue-properties-and-endurance-limits-of-stainless-steels/